

Mucoadhesive Poloxamer-Based Hydrogels for the Release of HP-beta-CD-Complexed Dexamethasone in the Treatment of Buccal Diseases

Raul Diaz-Salmeron, Balthazar Toussaint, Nicolas Huang, Etienne Bourgeois Ducournau, Gabriel Alviset, Sophie Goulay Dufay, Herve Hillaireau, Amelie Dufay Wojcicki, Vincent Boudy

▶ **To cite this version:**

Raul Diaz-Salmeron, Balthazar Toussaint, Nicolas Huang, Etienne Bourgeois Ducournau, Gabriel Alviset, et al.. Mucoadhesive Poloxamer-Based Hydrogels for the Release of HP-beta-CD-Complexed Dexamethasone in the Treatment of Buccal Diseases. Pharmaceutics, 2021, 13 (1), pp.117. 10.3390/pharmaceutics13010117 . hal-03291063

HAL Id: hal-03291063
https://cnrs.hal.science/hal-03291063

Submitted on 10 Sep 2021

HAL is a multi-disciplinary open access archive for the deposit and dissemination of scientific research documents, whether they are published or not. The documents may come from teaching and research institutions in France or abroad, or from public or private research centers.

L'archive ouverte pluridisciplinaire **HAL**, est destinée au dépôt et à la diffusion de documents scientifiques de niveau recherche, publiés ou non, émanant des établissements d'enseignement et de recherche français ou étrangers, des laboratoires publics ou privés.

pharmaceutics

MDPI

Article

Mucoadhesive Poloxamer-Based Hydrogels for the Release of HP-β-CD-Complexed Dexamethasone in the Treatment of Buccal Diseases

Raul Diaz-Salmeron [1,*], Balthazar Toussaint [1,2], Nicolas Huang [3], Etienne Bourgeois Ducournau [1], Gabriel Alviset [1], Sophie Goulay Dufaÿ [1], Hervé Hillaireau [3], Amélie Dufaÿ Wojcicki [1,†] and Vincent Boudy [1,2,†]

[1] Département de Recherche et Développement Pharmaceutique, Agence Générale des Equipements et Produits de Santé (AGEPS), 75005 Paris, France; balthazar.toussaint@aphp.fr (B.T.); ebourgeois@septodont.com (E.B.D.); gabriel.alviset@unither-pharma.com (G.A.); sophie.dufay@aphp.fr (S.G.D.); amelie.wojcicki@aphp.fr (A.D.W.); vincent.boudy@aphp.fr (V.B.)
[2] CNRS UMR 8258—Inserm U1022, Paris Descartes University, 75006 Paris, France
[3] Institut Galien Paris Saclay, Université Paris-Saclay, CNRS, 92296 Châtenay-Malabry, France; nicolas.huang@universite-paris-saclay.fr (N.H.); herve.hillaireau@universite-paris-saclay.fr (H.H.)
* Correspondence: raul.diazsalmeron@aphp.fr
† These authors contributed equally to this paper.

Abstract: Oral lichen planus (OLP) is an ongoing and chronic inflammatory disease affecting the mucous membrane of the oral cavity. Currently, the treatment of choice consists in the direct application into the buccal cavity of semisolid formulations containing a corticosteroid molecule to decrease inflammatory signs and symptoms. However, this administration route has shown various disadvantages limiting its clinical use and efficacy. Indeed, the frequency of application and the incorrect use of the preparation may lead to a poor efficacy and limit the treatment compliance. Furthermore, the saliva clearance and the mechanical stress present in the buccal cavity also involve a decrease in the mucosal exposure to the drug. In this context, the design of a new pharmaceutical formulation, containing a steroidal anti-inflammatory, mucoadhesive, sprayable and exhibiting a sustained and controlled release seems to be suitable to overcome the main limitations of the existing pharmaceutical dosage forms. The present work reports the formulation, optimization and evaluation of the mucoadhesive and release properties of a poloxamer 407 thermosensitive hydrogel containing a poorly water-soluble corticosteroid, dexamethasone acetate (DMA), threaded into hydroxypropyl-beta-cyclodextrin (HP-β-CD) molecules. Firstly, physicochemical properties were assessed to ensure suitable complexation of DMA into HP-β-CD cavities. Then, rheological properties, in the presence and absence of various mucoadhesive agents, were determined and optimized. The hydration ratio (0.218–0.191), the poloxamer 407 (15–17 wt%) percentage and liquid-cyclodextrin state were optimized as a function of the gelation transition temperature, viscoelastic behavior and dynamic flow viscosity. Deformation and resistance properties were evaluated in the presence of various mucoadhesive compounds, being the sodium alginate and xanthan gum the most suitable to improve adhesion and mucoadhesion properties. Xanthan gum was shown as the best agent prolonging the hydrogel retention time up to 45 min. Furthermore, xanthan gum has been found as a relevant polymer matrix controlling drug release by diffusion and swelling processes in order to achieve therapeutic concentration for prolonged periods of time.

Keywords: mucoadhesion; controlled-drug release; polysaccharides; poloxamers; cyclodextrins

check for updates

Citation: Diaz-Salmeron, R.; Toussaint, B.; Huang, N.; Bourgeois Ducournau, E.; Alviset, G.; Goulay Dufaÿ, S.; Hillaireau, H.; Dufaÿ Wojcicki, A.; Boudy, V. Mucoadhesive Poloxamer-Based Hydrogels for the Release of HP-β-CD-Complexed Dexamethasone in the Treatment of Buccal Diseases. *Pharmaceutics* **2021**, *13*, 117. https://doi.org/10.3390/pharmaceutics13010117

Received: 23 December 2020
Accepted: 12 January 2021
Published: 18 January 2021

Publisher's Note: MDPI stays neutral with regard to jurisdictional claims in published maps and institutional affiliations.

Copyright: © 2021 by the authors. Licensee MDPI, Basel, Switzerland. This article is an open access article distributed under the terms and conditions of the Creative Commons Attribution (CC BY) license (https://creativecommons.org/licenses/by/4.0/).

1. Introduction

Lichen planus (LP) is a chronic inflammatory dermato-mucosal disease affecting most frequently the skin and oral mucosa areas, and particularly involving the buccal mucous membrane. The pathology is called buccal or oral lichen planus (BLP or OLP). The nature

and origin of OLP are still unknown but various theories concerning its etiology have been proposed in the past [1,2]. That includes bacteria [3] or viral origin [4], neurogenic theories [5], environment or life-style factors [6] and other hypothesis associated with other diseases.

Currently, the treatment of choice for the OLP consists of the use of topical steroids. The use of many topical steroid compounds is widely described in the scientific literature. Thus, betamethasone [7], fluocinonide [8], hydrocortisone hemisuccinate [9], fluticasone [10] and other therapeutic molecules such as mometasone furoate [11], clobetasol propionate [12–15] or triamcinolone [16] demonstrated an improvement of signs (erythema, reticulation and ulceration) [17] and symptoms (pain and discomfort) [18].

However, existing topical steroid treatment has shown various disadvantages and limitations restricting their clinical use. Indeed, the frequency of application of corticosteroids limits the treatment compliance and makes it difficult to reach optimal effects. Thus, to achieve correct concentrations, the treatment may be applied between five to ten times daily [19], leading often to the ingestion of pharmaceutical preparations following incorrect use of the preparation [20]. Furthermore, the elderly, considered as a significant part of patients suffering OLP, found technically difficult to apply drug treatment to all locations of the buccal cavity, which means a lack of full contact between the drug and affected areas [21]. In addition, young people, with their current active lifestyle, need an effective and easy-to-apply treatment.

The permanent washing out of the buccal cavity by saliva also limits the average length of mucosal exposure to a drug treatment by three main mechanisms: drug dilution into the oral cavity, saliva clearance and mechanical stress due to swallowing and mastication processes [22].

In recent years, many dosage forms have been designed for buccal drug delivery in order to overcome the main limitations of this administration route [23–29]. Some interesting research work has been developed on thermosensitive poloxamer-based hydrogels, particularly with poloxamer 188 (P188) and 407 (P407). Indeed, thermosensitive hydrogels for buccal drug delivery have been designed and described in scientific literature [29–33]. These kind of hydrogels can undergo a sol–gel transition depending on the temperature [34,35]. Their chemical structure enables the self-association of hydrophobic poly(propylene oxide) (PPO) regions as micelles in an endothermic process [36,37], and subsequently the gelation, due to the formed micelle interactions, to form an elastic and three-dimensional network (solid-like). Thus, poloxamer-based hydrogels, and particularly P407, due to its colorless and washable properties [36], could be liquid at room temperature (20–25 °C) and is usually gelling between 30 and 35 °C. These thermosensitive properties make P407-based hydrogels appropriate for their use in buccal spraying devices [38] in order to reach an in situ gelation [39]. Additionally, these hydrogels are the most commonly used thermosensitive system in the pharmaceutical field [40–43] because they are not irritant for the skin and the mucous membranes. Nevertheless, poloxamer-based hydrogels exhibited very poor mucoadhesive properties once placed in the biological medium. Many strategies such as chemical modifications in poloxamer gels can be attempted. Thus, chemically-modified poloxamer gels have been already described in the literature to obtain improved mucoadhesive and mechanical properties [44,45]. Furthermore, physical strategies can be intended to reach acceptable mucoadhesive properties. Therefore, mucoadhesive agents or polymers have been used to improve the adhesive behavior of hydrogels. Anionic polymers, such as polyacrylic acid (PAA) and its derivatives (trade name carbomer) have been widely used because they exhibit excellent mucoadhesive characteristics due to the formation of strong hydrogen bonding interactions with the oligosaccharide chains of mucin [46–48]. Alginate, a naturally linear polysaccharide extracted from seaweed, bacteria and algae, has been also used for the preparation of mucoadhesive hydrogels [49,50]. In particular, high-molecular weight alginate, due to its flexibility properties, is able to bridge distant mucin sites causing the protein contraction and its mucoadhesive effect [48,51]. Xanthan gum (XG), another anionic polysaccharide, is widely used in the pharmaceutical and cosmetic industry for its

mucoadhesive properties [25,52]. This polysaccharide also generates a viscous medium slowing drug release in sustained release formulations [53–55].

Since the management of OLP treatments can vary considerably due to the lack of official guidelines [20], the treatment may be adjusted in the function of the disease stage for individual patients [56,57]. Dexamethasone, a class II steroidal anti-inflammatory, less potent than clobetasol but with less side effects, could be used for this purpose. Indeed, a drug delivery improvement of a dexamethasone formulation may be particularly useful for its clinical use even for other pathologies than OLP.

In this context, the aim of this experimental study was to formulate a hydrophobic and practically insoluble in water API [58,59], dexamethasone acetate (DMA), widely known for its anti-inflammatory properties [60–62], into a thermosensitive P407-based hydrogel containing different mucoadhesive agents, such as carbomer, sodium alginate or xanthan gum, to improve their interactions with mucins present at the buccal surface mucosa.

The main novelty of this study was the use of cyclic oligosaccharides to improve DMA solubility into a hydrogel. Due to the hydrophobic nature of DMA, the solubilization into an aqueous hydrogel is not adapted. To solve this problem, DMA molecules were previously complexed into the cavity of cyclodextrin molecules (CD), particularly into HP-β-CD, the most successful β-CD derivative to date [59,63,64]. CD compounds, produced by enzymatic degradation of starch [65] are able to form inclusion complexes with water-insoluble API due to different supramolecular forces such as Van der Waals or hydrophobic interactions [66]. CD molecules were of interest given the presence of hydrophilic groups on the outside, which is useful for maintaining the hydrophilicity and swelling behavior of the hydrogel. Their hydrophobic cavity enables and improves the entrapment, the apparent solubility and the controlled-release of hydrophobic drugs [34].

This paper describes for the first time the design of a novel thermosensitive hydrogel for buccal drug delivery intended to be sprayable (presenting a dynamic viscosity of less than 200 mPa.s at room temperature in order to suit for the identified device), and exhibiting an optimized sol–gel transition temperature (30–32 °C) that could allow the in situ gelation once administered in the oral cavity for the treatment of inflammatory diseases. Furthermore, satisfactory mucoadhesive properties and sustained and controlled drug release were obtained. In this paper, we focused on the formulation process of hydrogels and the mechanism of DMA encapsulation into HP-β-CD molecules and the rheological characterization of hydrogels and sustained-release. This paper describes for the first time the use of a CD complexed anti-inflammatory active substance contained in a mucoadhesive polymer matrix for the treatment of buccal diseases as OLP. Designing a specific formulation for the oral mucosa should improve the treatment efficiency due to a better absorption and the patient compliance due to an appropriate formulation.

2. Materials and Methods

2.1. Materials

Dexamethasone acetate was purchased from Aventis (Gentilly, France). Kolliphor-P407 was from BASF (Mississauga, Canada). Hydroxy-propyl-beta-cyclodextrin was purchased from Roquette (Paris, France). Mucoadhesive agents used in the experiments were xanthan gum (Satiaxane from Cargill, Puteaux, France), carbomer (Carbopol C971P from Lubrizol, Brussels, Belgium) and sodium alginate (Protanal LF 10/60 FT from FMC Biopolymer, Cork, Ireland). Porcine gastric mucin type II was from Sigma Aldrich (Saint-Louis, MO, USA). All the experiments were performed using sterile water from Fresenius Kabi (Sévres, France).

For the HBSS medium preparation, the chemical products used were calcium chloride × $2H_2O$, potassium chloride, potassium hydrogen phosphate anhydrate, sodium chloride, disodium dihydrogen phosphate × H_2O, sodium hydrogen carbonate, magnesium chloride × $6H_2O$ and magnesium sulfate × $7H_2O$. All these products were purchased from Sigma Aldrich (Saint-Louis, MO, USA).

2.2. Methods

2.2.1. Preparation of Hydrogels

Hydrogels were prepared according to the method called the "cold method" [36,67]. Concentrations of all components reported in this article were expressed as the weight/weight ratio (%*w*/*w*). The formulations were prepared following two different approaches. In both approaches the strategy was to form inclusion complexes between DMA and HP-β-CD in order to increase the apparent solubility of DMA. Indeed, its low aqueous solubility is limiting its clinical usefulness [68].

The first approach consisted of solubilization under magnetic stirring at 400 rpm at 4 °C of amounts of P407 (15–17% weight/weight (*w*/*w*)) in 20 g of distilled water containing the corresponding mucoadhesion agent previously dissolved (at 0.1 and 0.5% *w*/*w* for Carbopol C971P and sodium alginate and 0.05 and 0.1% *w*/*w* for the xanthan gum). At the same time, a second aqueous solution was prepared by adding amounts of HP-β-CD and DMA (0.1% *w*/*w*) in 30 g of distilled water under magnetic stirring at 400 rpm at room temperature. The first solution containing the dispersed amount of P407 was completed with the total volume of the second aqueous solution. The final solution was allowed to stir at 400 rpm for 24 h at 4 °C in order to stay in the solution state of the thermogelling agent P407 and not to disadvantage the homogeneity of the preparation. After 24 h, the total formulation weight was adjusted to 100 g by adding distilled water and stirring for 5 min.

For the second approach, mucoadhesion agent was totally dissolved in 20 g of sterile water under magnetic stirring at 400 rpm. Then, the corresponding amount of P407 was progressively and gradually added. The final weight of the aqueous solution was completed with 20 g of sterile water. This solution was allowed to rest at 4 °C for 24 h. A second aqueous solution was prepared by dissolving amount of HP-β-CD in 30 g of sterile water under magnetic stirring at 400 rpm during 5 min. For the formulations containing the API (0.1% *w*/*w*), the exact amount of DMA was added and allowed to stir for 1 h at 400 rpm then ultrasonicated during 2 min.

Once, the formulation approach influence was investigated, the first method was retained for the characterization of physicochemical properties of hydrogels and in vitro dissolution studies. Table 1 summarizes quantitative and qualitative composition of hydrogels tested.

Table 1. Qualitative and quantitative composition of hydrogels.

	P407 (wt%)	P407/H_2O Ratio	H_2O (wt%)	HP-β-CD (wt%)	DMA (wt%)	MA Agent	MA (wt%)	Use
A	17.00	83.00	0.205	0	-	-	-	Physicochemical characterization
B	17.00	78.13	0.218	4.87	-	-	-	Physicochemical characterization
C	16.17	78.96	0.205	4.87	-	-	-	Physicochemical characterization
D	15.21	79.82	0.191	4.87	0.10	-	-	Physicochemical characterization
E	16.16	78.87	0.205	4.87	0.10	-	-	Physicochemical characterization
F	15.21	79.82	0.191	4.87	0.10	Carbopol 971P	0.10	MA in vitro tests and in vitro dissolution profile
G	15.21	79.82	0.191	4.87	0.10	Carbopol 971P	0.50	MA in vitro tests and in vitro dissolution profile
H	15.21	79.82	0.191	4.87	0.10	Sodium alginate	0.10	MA in vitro tests and in vitro dissolution profile
I	15.21	79.82	0.191	4.87	0.10	Sodium alginate	0.50	MA in vitro tests and in vitro dissolution profile
J	15.21	79.82	0.191	4.87	0.10	Xanthan Gum	0.05	MA in vitro tests and in vitro dissolution profile
K	15.21	79.82	0.191	4.87	0.10	Xanthan Gum	0.10	MA in vitro tests and in vitro dissolution profile

2.2.2. Phase Solubility Diagrams and Apparent Solubility Determination

Phase solubility studies were carried out according to the method described by Higuchi and Connors [69]. An excess of DMA (50 mg corresponding to 0.1% m/v) was added in a glass vial containing 50 mL of an aqueous solution of HP-β-CD at concentrations ranging from 0.46 to 23 mM representing 1/0; 1/0.2; 1/0.4; 1/1; 1/2; 1/4 and 1/10 molar ratios (DMA/HP-β-CD). Vials were kept under magnetic stirring at 400 rpm at room temperature for 72 h (duration estimated to be enough to reach the complexation equilibrium). The intrinsic solubility of DMA in sterile water was determined using the same protocol without the presence of cyclodextrin molecules. Then the samples were filtered through a 0.22 µm membrane filter and diluted 1/20 for UV spectrophotometric determination at a wavelength of 242 nm. Absorbance of different sample ratios was transformed in molar concentrations using a standard curve.

The standard curve was prepared in an aqueous solution of DMA/HP-β-CD using a stock solution containing 1.15 mM (25 mg) and 19.2 mM (1350 mg) of DMA and HP-β-CD respectively. The concentration of DMA should be below the solubility of the inclusion complexes. The stock solution was diluted 1/20 with sterile water then diluted again to obtain valid concentrations for quantification ranging from 0.058 to 0.012 mM. In order to evaluate the matrix effect of HP-β-CD, another standard curve using a stock solution of DMA in propylene glycol (PG) was prepared in the same range of concentrations because of the total solubility of DMA in PG. The equations of the calibration curves were $y = 13.492x + 0.0126$, $r^2 = 0.999$ and $y = 15.046x - 0.0065$, $r^2 = 0.998$ in an aqueous solution of HP-β-CD and PG, respectively.

Slope values of each calibration curve were compared to investigate this effect.

2.2.3. Rheological Characterization of Formulations

All the rheological studies were carried out on an Anton Paar MCR102 Rheometer (Graz, Austria). The geometry chosen was a stainless steel cone/plate equipped with a solvent trap (diameter 50 mm, angle 1° and truncation 100 µm) providing a homogeneous shear of the samples. All the data obtained were analyzed using the Anton Paar RheoCompass™ software version 1.25 (Graz, Austria) associated to the rheometer. All experiments were performed in triplicate and all data are expressed as the mean ± standard deviation.

Flow Rheometry Studies

Continuous shear analysis of formulations was performed at 25 and 37 °C using a stress sweep. Samples were carefully placed onto the inferior plate and allowed to equilibrate for at least 2 min prior to analysis. Flow curves were measured over shear rates ranging from 0.1 to 1000 s^{-1}. The shear rate was firstly increased over a period of 60 s (upward curve), held at the upper limit for 30 s and subsequently decreased gradually to the lower limit over a period of 60 s (downward curve).

In each case, the continuous shear properties of at least three replicates were determined and the descending flow curves were fitted to a Carreau–Yasuda model equation [70] as follows:

$$n = n_\infty + (n_0 - n_\infty) \times \left[1 + \left(\lambda\dot{\gamma}\right)^a\right]^{(n-1)/a} \quad (1)$$

where η is the viscosity, $\dot{\gamma}$ is the shear rate, η_0 is the limiting steady state viscosity at the zero shear rate, η_∞ is the limiting steady state viscosity at the infinite shear rate, n is the power index and confers a power-law behavior to the curve, a is the Yasuda exponent describing the transition from the first Newtonian plateau to the power-law behavior and λ is the time constant setting the position of the power-law behavior as a function of the shear rate.

Oscillatory Rheometry Studies and Determination of Gelation Transition Temperature

A sinusoidal shear was applied to the sample in order to determine the storage (or elastic) modulus G' and the loss (or viscous) modulus G''. The stress τ (t) and the strain γ (t) were defined as follows in the Equations (2) and (3):

$$\tau\ (t) = \ \tau_0 \cos(\omega t) \tag{2}$$

$$\gamma\ (t) = \ \gamma_0 \cos(\omega t - \ \delta) \tag{3}$$

where τ_0 and γ_0 are the maximal amplitudes of stress and strain respectively, ω is the shear pulsation ($\omega = 2\pi N$; N = frequency) and δ is the phase angle stress/strain.

The phase angle between stress and strain will define the storage (G') and the loss (G'') moduli as follows in Equations (4) and (5):

$$G' = \ \frac{\tau_0}{\gamma_0} \cos \delta \tag{4}$$

$$G'' = \ \frac{\tau_0}{\gamma_0} \sin \delta \tag{5}$$

After performance of an amplitude sweep (f = 1 Hz) and a frequency sweep (γ = 0.1%), the linear viscoelastic region (LVR) was estimated. All subsequent measurements of the storage modulus (G') and loss modulus (G'') were run within the LVR at an amplitude of 0.1% and a frequency of 1 Hz, where G' and G'' remained invariant and the sample did not undergo structural modifications.

The determination of the gelation transition temperature ($T_{sol–gel}$) of formulations was performed using the previously described conditions carrying out a temperature sweep analysis over temperatures ranging from 20 to 40 °C and a heating rate of 1 °C/min.

2.2.4. Measurement of the Adhesive and Mucoadhesive Forces

The adhesive and mucoadhesive behavior of formulations presenting different mucoadhesive agents (Carbopol C971P (carbomer), Protanal LF 10/60 FT (sodium alginate) and Satiaxane (xanthan gum)) were evaluated by measuring the force and the work required to detach the corresponding formulation from the upper plate of the rheometer in a tensile test. This test was carried out with an Anton Paar MCR102 Rheometer and the raw data were analyzed using the Anton PaarRheoCompass software. The geometry chosen to perform all the experiments was a stainless-steel plate/plate (diameter = 50 mm).

For adhesion experiments, the hydrogel was carefully loaded on the lower plate of the rheometer and heated at 37 °C for ensuring the gelation of the system. After that, the upper plate was lowered until contact with the sample (100 µm). After a contact time of 1 min with the hydrogel with a contact force of 0.3 N, the upper plate (rheometer mobile) was moved upward at a constant speed of 5000 µm/s. The strength was recorded as a function of the displacement (elongation), which allowed us to determine the maximal detachment force (F_{adh}) and the work of adhesion (W_{adh}), calculated by determining the maximal peak and the area under the curve from the force–elongation curve.

For mucoadhesion experiments, 5% (w/v) porcine gastric mucin dispersion was previously prepared in sterile water. Mucin films were prepared directly on the upper plate of the rheometer. The mucin dispersion (300 µL) was placed and spread homogeneously on the rheometer mobile and heated during 15 min at 37 °C in the oven allowing the mucin dispersion to dry. Then the hydrogel was loaded on the lower plate and the rheometer mobile was brought to contact under the same experimental conditions as described above for adhesion experiments.

2.2.5. Flow-Through USP-4 Apparatus In Vitro Drug Release

Dexamethasone acetate (DMA) release from P407-HP-β-CD hydrogels was evaluated at 37 °C using an USP-4 apparatus Sotax CE7 Smart (Sotax AG, Nordring, Switzerland) equipped with 22.6 mm diameter cells [71,72]. A ruby bead (5 mm diameter) was placed at the base of the sample cell. Of the hydrogel sample 0.5 g were placed in a Float-A-Lyzer and then inserted in the USP-4 cell. To fill the bottom conical part of the sample cell, 4 g of 1 mm glass beads were added. Of HBSS buffer (pH = 6.8) 50 mL maintained at 37 °C were used as release media in these studies (final concentration of DMA in the release media was 10 µg/mL, corresponding to 100% of drug release). The media was perfused in a closed-loop setting at 8 mL/min. The released DMA amount was monitored every 3 min by UV absorption at 242 nm as the wavelength. An equal amount of DMA complexed with HP-β-CD in solution (10 µg/mL) was placed in the release media directly as a control sample of the complete release of DMA from hydrogel formulations. The cumulative release (%) of DMA from hydrogels was calculated by dividing the DMA amount released from the hydrogel formulation by the measured amount of released DMA from the control solution.

To compare dissolution profiles, the difference factor (f_1) and similarity factor (f_2) were determined for each hydrogel formulation release profile, comparing them to the free mucoadhesive dissolution profile [73,74]. The f_1 and f_2 factors provide an independent-model method for data analysis to measure the similarity between two release profiles.

The factor f_1 is the percentage of difference between two dissolution profiles at each time point and is calculated using the following expression:

$$f_1 = \{[SH|R_t - T_t|]/SHR_t\} \times 100 \quad (6)$$

where R_t is the amount of released drug on the reference formulation and T_t is the amount of released drug on the test formulation. If the release profiles are completely superimposed, the f_1 factor reaches a value of 0. From a practical point of view, values between $0 \leq f_1 \leq 15$ could be considered as superimposed release profiles.

The factor f_2 is calculated using the following expression [75,76]:

$$f_2 = 50 \times \log\left\{\left[1/1 + \left(SH\,(R_t - T_t)^2\right)/N\right]^{-0.5} \times 100\right\} \quad (7)$$

where N is the number of experimental data values. If the profiles are completely superimposed, the f_2 factor reaches a value of 100. From a practical point of view, values between $50 \leq f_2 \leq 100$ can be considered as superimposed release profiles.

2.2.6. Statistical Analysis

Statistical analyses were performed using Prism version 7.0 software (GraphPad, Northside, CA, USA). Normality of experiment data was examined using a Shapiro–Wilk test. A one-way analysis of variance test (ANOVA) followed by a Tukey's multiple comparison post-test comparing means between different groups were performed. The level of statistical significance was set at p-value < 0.05.

3. Results and Discussion

3.1. Influence of the Hydrogel Preparation Approach on the Physicochemical Behavior of Hydrogels

Both hydrogel preparation approaches were inspired in the called "cold method" consisting of the solubilization of P407 chains at 4 °C for 24 h [36,67]. To improve and facilitate the dispersion of poly(ethylene oxide)-poly(propylene oxide)-poly(ethylene oxide) (PEO-PPO-PEO) polymer chain blocks, the P407 powder was dispersed in a first volume of sterile water then in a second one. In the first approach, this second volume added consisted of an aqueous solution containing complexes of DMA and HP-β-CD molecules but also in a small amount their free-complexed state (Figure 1). The resulting solution was stored for 24 h at 4 °C. At this moment, supramolecular interactions between hydrophobic

regions of P407 and HP-β-CD cavities may exist leading to the formation of PPO-HP-β-CD inclusion complexes and the non-complexation of DMA molecules, even relocation of the DMA [77–79]. Indeed, when this solution is left at room temperature (15–20 °C), molecules of DMA are precipitated leading to a white coloration of the anterior limpid preparation (DMA is not anymore complexed and not soluble in water in its free state). At these levels of temperature, P407 micelles could not be correctly self-assembled in the presence of HP-β-CD leading to the formation of a very weak hydrogel whereas P407 is shared between CD and other P407 molecules therefore in too small of an amount.

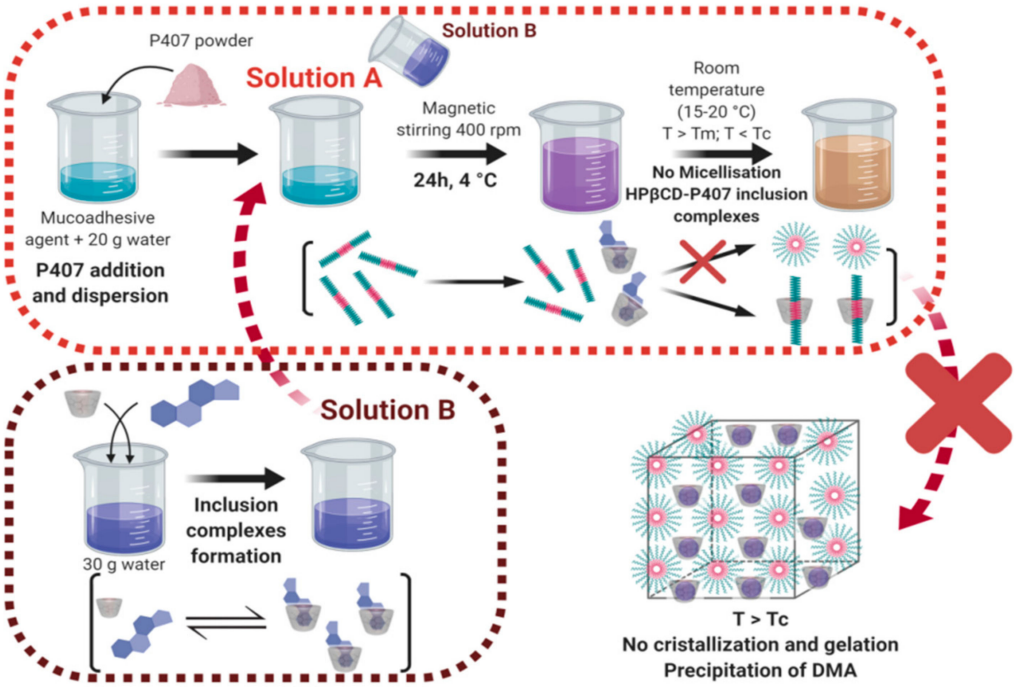


Figure 1. Schematic representation of the association of poloxamer P407 with HP-β-CD dethreading the inclusion complexes previously formed with DMA in sterile water.

For the second approach, the P407 dispersion was completed with a second volume of distilled water and stored at 4 °C under magnetic stirring overnight to solubilize all the polymers chains (Figure 2). The following day this solution was placed at room temperature (15–20 °C) in order to obtain the micellization process. After that, DMA-HP-β-CD solution was added and the resulting solution was heated at 30 °C to allow the gelation process. The DMA-HP-β-CD solution was prepared 3 days before. FT-IR and X-ray diffraction patterns reported in the scientific literature demonstrated the formation of DMA-HP-β-CD inclusion complexes [80]. The final product obtained was a strong hydrogel without any DMA precipitation. In this second approach, the prior micelle formation avoided the formation of inclusion complexes between PPO blocks of P407 and HP-β-CD.

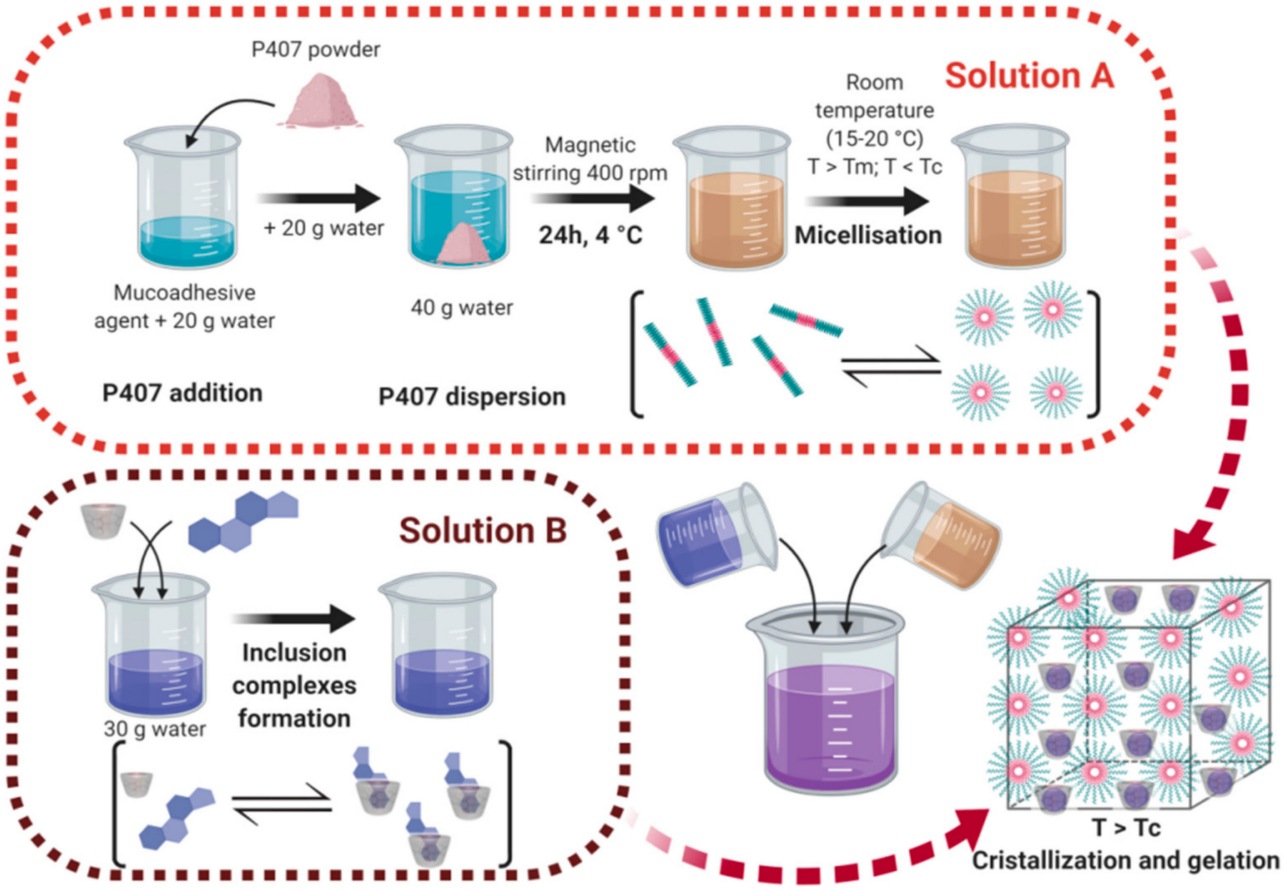


Figure 2. Schematic representation of the self-association of poloxamer 407 and complexation of HP-β-CD with DMA in sterile water to form poloxamer P407-based hydrogels.

3.2. Phase Solubility Diagrams and Apparent Solubility Determination

The influence of the presence of HP-β-CD in the solubilization of DMA was investigated by adding an excess of DMA powder in different vials containing increasing concentrations of HP-β-CD and allowing to stir during 72 h to reach the complexation equilibrium. Previous empirical studies have already demonstrated by ^{1}H-NMR and ITC that dexamethasone phosphate (DMX) interacts with HP-β-CD molecules to form stable inclusion complexes after 3 days [81–83].

The standard curve was prepared in an aqueous solution of DMA-HP-β-CD because of the matrix effect highlighted (data not shown). Indeed, molar extinction coefficient values were different for a propylene glycol or aqueous HP-β-CD standard curve (data not shown). For the standard curve DMA and HP-β-CD were used at concentrations of 1.15 mM and 19.2 mM respectively. These molar concentrations were selected through a prior standard curve in propylene glycol, ensuring the total dissolution of DMA in the HP-β-CD aqueous solution.

Phase solubility diagrams at different HP-β-CD concentrations (Figure 3) were obtained in order to evaluate the apparent solubility of DMA.

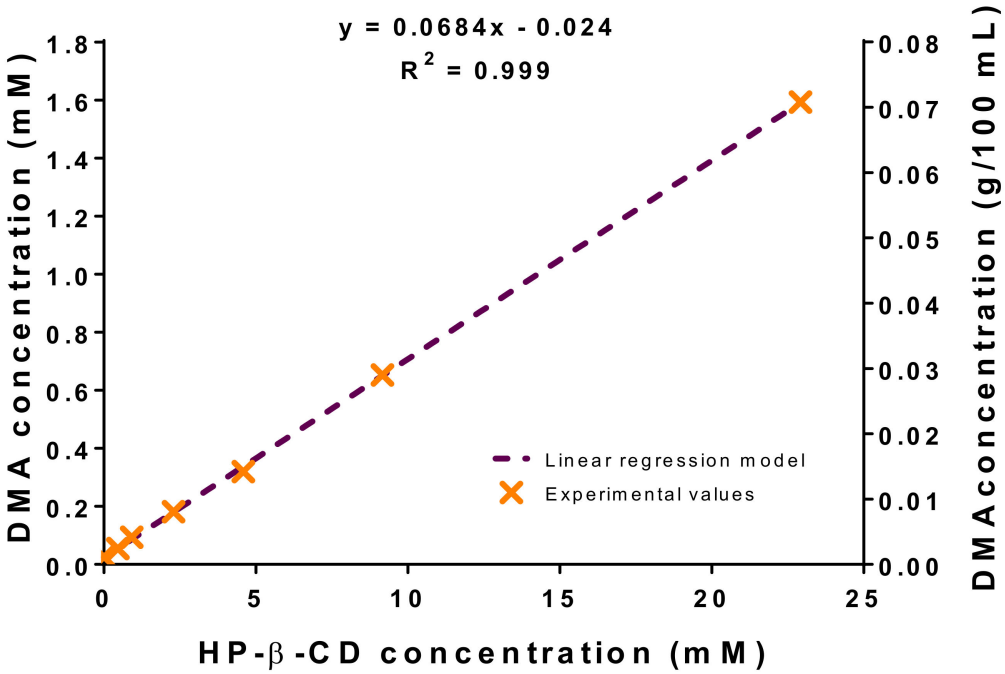


Figure 3. Experimental phase solubility diagram of DMA for HP-β-CD (n = 3).

The analysis of these diagrams could give an overview of the process of complexation between DMA and cyclodextrin (CD) molecules based on Higuchi and Connors classification (69). Thus, there are two mains groups describing the relationship between the increasing dissolved drug concentration when CD concentration is increased: A-type and B-type. A-type phase-solubility curves exhibit increased drug solubility by increasing CD concentration. The increased solubility can be linear with the increasing host concentration (A_L-type) or can present negative or positive deviations (A_N- and A_P-type) from the linearity explained by the self-association or aggregation of the cyclodextrin molecules or their complexes. For B-type, the phase-solubility diagrams of the formed-complexes show a limited solubility in the aqueous solution or suspensions. Thus, B_S-type exhibited reduced solubility with a maximal solubility in a concentration plateau. B_I-type shows insolubility profiles at all the concentrations in the aqueous medium [84].

Higuchi and Connors phase-solubility diagram [69] showed a linear increase in DMA solubility as a function of HP-β-CD concentration, suggesting the formation of 1:1 inclusion complexes between HP-β-CD and DMA (A_L-type) [85,86]. Without any further additional information, it is usually made that the assumption of 1:1 complex stoichiometry meaning that one molecule of HP-β-CD is complexing one molecule of DMA. However, the A_L diagram means that only one molecule of HP-β-CD is involved in the interaction with one or more DMA molecules. These results are in agreement with other empirical studies. Indeed, ITC titration profiles reported in the scientific literature showing exothermic heats highlighting the interaction between β-CD molecules and DMA. The corrected heat of reaction per mole curves showed also a very good fit with a 1:1 binding stoichiometry model [82,87]. In addition, the same study reported the Job's plots showing the intersection of two lines at a mole fraction of 0.52, which corresponds to a 1:0.92 binding stoichiometry [82,87].

A more quantitative description of the complexation behavior can be achieved by considering the value of the binding constant (also called stability constant or complex equilibrium constant) calculated according to the Equation (8) and assuming a 1:1 interaction stoichiometry:

$$k_{1:1} = \frac{slope}{S_0\,(1 - slope)} \quad (8)$$

where $k_{1:1}$ is the calculated constant from the slope of the phase-solubility diagram, S_0 is the intrinsic solubility of the drug in the absence of HP-β-CD molecules (this value

should be equivalent to the S_{int}, which corresponds to the y-intercept value of the phase solubility plot in the linear region). In our study the value of $k_{1:1}$ was 3124 M^{-1}, a little higher than in the literature [66,87–89]. This value of stability constant is very high and corroborates that, once the inclusion complexes are formed, they are relatively stable, confirming that the second method of preparation of hydrogels is the most suitable to obtain stable formulations. Values of $k_{1:1}$ between 200 and 5000 M^{-1} are considered as the most suitable to improve the bioavailability of poorly water soluble drugs [80,90].

The complexation of DMA in HP-β-CD led to the increase of the apparent solubility of DMA. The presence of HP-β-CD molecules allowed it to reach a DMA concentration of 1.6 mM, representing an apparent solubility enhancement factor of 67 (S_0 = 0.024 mM [91,92]. The complexation efficiency (CE) was also calculated from Equation (9), giving a value of 0.075.

$$CE = S_0 k_{1:1} = \frac{[DMA][HP-\beta-CD]}{HP-\beta-CD} = \frac{slope}{(1-slope)} \quad (9)$$

The main goal of phase-solubility diagrams was to investigate the interaction stoichiometry and the HP-β-CD concentration necessary to reach a DMA apparent solubility of 2.30 mM (0.10% w/v). According to the phase-solubility plot, the HP-β-CD threshold concentration to reach it was 33.6 mM (4.54% w/w). This HP-β-CD concentration was kept for the next experiments.

3.3. Rheological Studies

The ideal candidate for the controlled delivery of an API to the buccal cavity should exhibit a wide variety of characteristics mainly including the ease of application, the low elimination and the high retention time into the cavity once the drug is administered. For these reasons, rheological characterization seems to be essential to select the ideal product profile. Tables 2 and 3 show the compositions and the main rheological parameters obtained for the different formulations.

Table 2. Composition of poloxamer P407-based hydrogels in the presence and absence of HP-β-CD and DMA. Values of the storage (G') and loss (G'') moduli, tan δ at 20 and 37 °C, viscoelastic behavior before and after gelation and $T_{sol-gel}$ for poloxomer P407-based hydrogels without mucoadhesive agents. Data were reported as the mean ± SD (n = 3).

		Without DMA			**With DMA**	
		A	**B**	**C**	**D**	**E**
HP-β-CD (wt%)		0	4.87	4.87	4.87	4.87
P407 (wt%)		17	17	16.17	15.21	16.16
H_2O (wt%)		83.00	78.13	78.96	79.82	78.87
P407/H_2O ratio		0.205	0.218	0.205	0.191	0.205
DMA (wt%)		Ø	Ø	Ø	0.1	0.1
20 °C	G' (Pa)	0.07 ± 0.08	0.35 ± 0.56	0.02 ± 0.03	0.08 ± 0.08	0.05 ± 0.08
	G'' (Pa)	0.23 ± 0.03	0.26 ± 0.01	0.20 ± 0.01	0.17 ± 0.06	0.31 ± 0.14
37 °C	G' (Pa)	12139 ± 329	10540 ± 291	8052 ± 566	3787 ± 960	9904 ± 641
	G'' (Pa)	1419 ± 987	772 ± 282	906 ± 27	924 ± 111	1001 ± 44
tan δ at 20 °C		0.32 ± 0.45	1.31 ± 2.06	0.08 ± 0.14	0.36 ± 0.38	0.21 ± 0.37
tan δ at 37 °C		11.47 ± 6.58	14.79 ± 4.69	8.89 ± 0.63	4.05 ± 0.60	9.89 ± 0.45
$T_{sol-gel}$ (°C)		26.4 ± 0.5	28.8 ± 0.0	29.7 ± 0.6	30.2 ± 0.4	27.9 ± 0.6

Table 3. Values of the storage (G') and loss (G'') moduli, tan δ at 20 and 37 °C, viscoelastic behavior before and after gelation and $T_{sol–gel}$ for poloxomer P407-based hydrogels containing various mucoadhesive agents. Data were reported as the mean ± SD (n = 3).

		Without Mucoadhesive	Mucoadhesive Agents					
		D	F	G	H	I	J	K
		Control sample	Carbopol 971P		Sodium alginate		Xanthan Gum	
			0.1%	0.5%	0.1%	0.5%	0.05%	0.1%
20 °C	G' (Pa)	0.02 ± 0.02	0.03 ± 0.03	-	0.08 ± 0.07	0.09 ± 0.17	0.29 ± 0.02	0.61 ± 0.09
	G'' (Pa)	0.25 ± 0.14	0.33 ± 0.04	-	0.28 ± 0.07	0.69 ± 0.18	0.45 ± 0.16	0.87 ± 0.46
37 °C	G' (Pa)	3810 ± 385	1204 ± 14	-	1123 ± 132	1198 ± 107	1528 ± 99	1209 ± 233
	G'' (Pa)	1073 ± 51	169 ± 69	-	150 ± 6	220 ± 36	369 ± 44	215 ± 79
tan δ 20 °C		13.92 ± 3.85	10.62 ± 3.60	-	3.62 ± 0.12	7.13 ± 0.18	1.60 ± 0.66	1.43 ± 0.70
tan δ 37 °C		0.28 ± 0.02	0.14 ± 0.06	-	0.13 ± 0.01	0.18 ± 0.04	0.24 ± 0.02	0.17 ± 0.03
$T_{sol–gel}$ (°C)		30.5 ± 0.4	30.8 ± 0.6	-	30.2 ± 0.3	31.0 ± 0.2	29.7 ± 0.6	29.6 ± 0.5

ND: not determined, sample G exhibited an elastic behavior (solid-like) at room temperature, without a mucoadhesive agent.

3.3.1. Oscillatory Rheometry Studies

Oscillatory studies were performed in order to determine G', G'' and tan δ in the LVR of different formulations. Concerning the two dynamic moduli acquired, the higher the G' value is, the more expanded the elastic behavior is. In the other hand and conversely, the higher the G'' is, the more pronounced the viscous behavior is. We can usually consider that one formulation exhibits a viscous-dominant behavior (liquid-like) when the G'' value is higher than the G' value. Contrarily, when the G' value is higher than the G'' value, the formulation exhibits an elastic-dominant behavior (solid-like) at a given oscillatory frequency. The G''-to-G' ratio gives tan δ, which is a measure of the relative contribution of the viscous behavior to the mechanical properties of materials. A gel (solid-like) state is observed when tan $\delta \leq 1$ [36,93].

G' and G'' dynamic moduli were used to determine the $T_{sol–gel}$ of formulations. Indeed, the temperature corresponding to the crossover of the elastic and viscous moduli was considered as the gelation transition temperature (Figure 4).

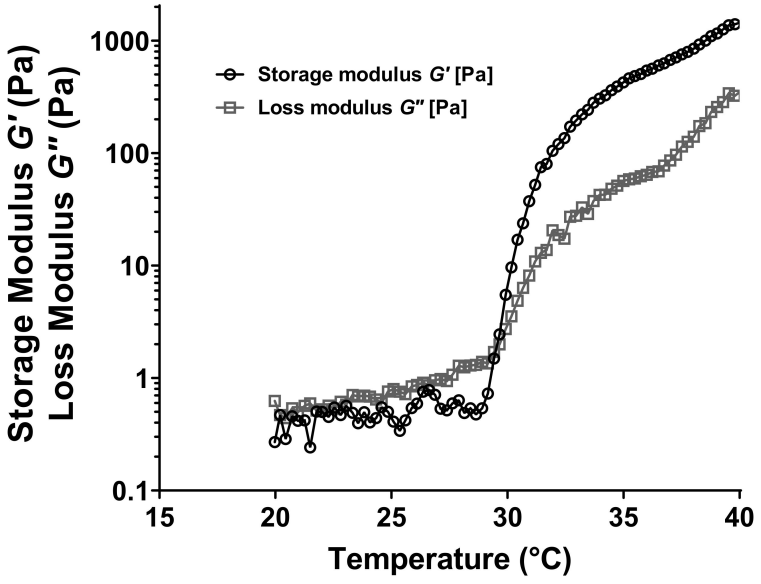


Figure 4. Typical profile of the variation of the storage (G') and loss (G'') moduli as a function of temperature. Experiments performed with a poloxamer P407-based hydrogel at 16% (w/w) containing xanthan gum at a concentration of 0.1%, sample K (w/w).

The possible effect of HP-β-CD molecules and the hydration ratio of P407 polymer chains were investigated by comparing the viscoelastic properties and $T_{sol–gel}$ of formulations A, B and C (Table 2). Comparative analysis between formulations A and B (equal mass ratio) and A and C (equal hydration ratio) highlighted the significant increase of gelation transition temperature when HP-β-CD was added (p-value = 0.0008 and <0.0001 for the comparison between formulation A and formulation B and C respectively after a one-way ANOVA test). Indeed, the flow heat provided to form the gel needs to be more important than previously described, because HP-β-CD molecules are located between P407 polymer chains, leading to a steric blockage. In one hand, the heat supplied to self-assemble P407 polymer chains in micelles may be higher, leading to an increase of the critical micellization temperature (CMT). In the other hand, once the micelles of P407 are well-formed, the HP-β-CD hindered molecules decrease the micelle interactions between themselves [94,95]. That will result in an increase of the crystallization temperature. Comparative analysis of formulations B and C (equal HP-β-CD but different hydration ratio) confirmed that the hydration ratio of P407 polymer chains plays an essential role in the sol–gel transition. Indeed, the higher the hydration ratio is, the higher the $T_{sol–gel}$ will be. The formulation C, showing a hydration ratio more important than the formulation B, exhibited a higher $T_{sol–gel}$. The heat provided to induce the gelation need to be higher because water molecules in the micellar core are increased and the micellization is disfavored, leading to an increase in the CMT and subsequently in the $T_{sol–gel}$ [93].

The influence of the DMA addition in the viscoelastic properties of hydrogels was evaluated by comparing the $T_{sol–gel}$, G' and G'' of formulations D and E with a control sample without active substance (formulation C), as reported in Table 2. Since the water-soluble complexes formed between HP-β-CD and DMA are not expected to enter into the hydrophobic region of poloxamer micelles, the hypothesis is that the inclusion complexes would be located in the aqueous region of hydrogels. Indeed, when cyclodextrin molecules are added on the complexed-state with DMA molecules (formulation E), those ones may interact less with hydrophobic blocks of PPO P407 chains, favoring the micellization and crystallization of P407 polymer chains. That may reduce the $T_{sol–gel}$, as we can observe the results shown in Table 2. However, when CD molecules are added in their free-complexed state (formulation C), they may establish more interactions with hydrophobic poloxamer block chains, leading to an increase on the transition temperature (p-value = 0.0064 for the comparison between formulations C and E after a one-way ANOVA test).

Hydration ratio of P407 was firstly identified as a key parameter controlling the viscoelastic properties of formulations. In order to retrieve an equivalent $T_{sol–gel}$, the hydration ratio of formulation E was decreased (formulation D), and the initial transition temperature without active substance was recovered (p-value = 0.0011 for the comparison between formulation D and E after a one-way ANOVA test). Thus, the formulation D, containing a hydration ratio of 0.191 was kept for experiments in the presence of mucoadhesive agents.

The effect of mucoadhesive agents on the viscoelastic properties of P407-based hydrogels was also investigated (Table 3). The transition temperature did not significantly change whatever the mucoadhesive agents used (p-value > 0.05 for the comparison between all the formulations containing mucoadhesive agents (samples F-K) and the control sample (sample D) after a one-way ANOVA test). All the mucoadhesive hydrogels showed $T_{sol–gel}$ above 29.5 °C and very close to the control sample (formulation D, without mucoadhesive agent). However, regarding the elastic modulus values at 37 °C, we could find significantly lower values than the control sample, suggesting the unfavorable interaction between the mucoadhesive agent and P407-hydrogel (p-value < 0.0001). The mucoadhesive properties of hydrogels containing a mucoadhesive agent need to be investigated to justify the addition of those products in the formulations [96].

3.3.2. Flow Rheometry Studies

Viscosity and flow properties were performed at 25 and 37 °C and were shown in Figure 5. These properties may determine the ease of administration of the product into the buccal cavity (generally at room temperature) by spraying and the time-dependent clearance of the formulation after the administration (at physiological temperature).

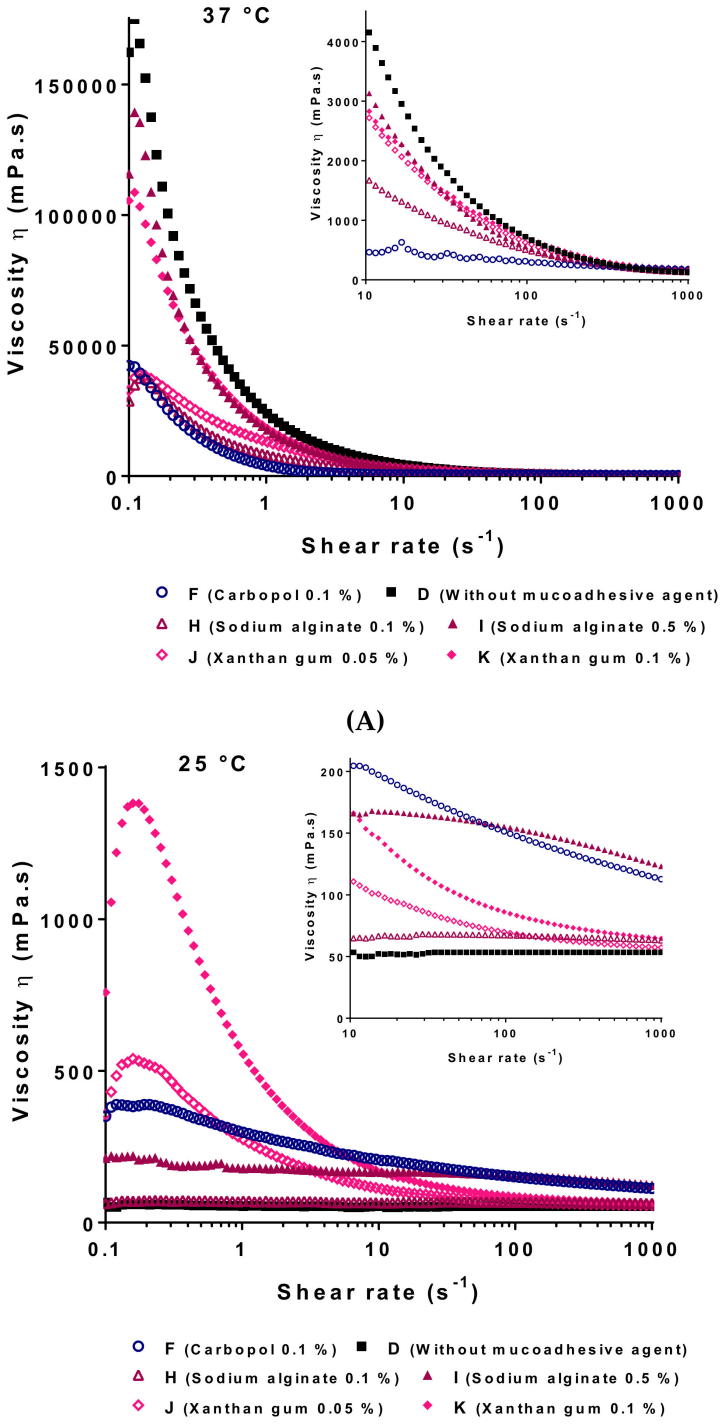


Figure 5. Dynamic viscosity as a function of shear rate at 37 (**A**) and 25 °C (**B**) of various poloxamer P407-based hydrogels. The mean of 3 experiments are represented.

In both cases, 25 and 37 °C, all the formulations, except the control sample without mucoadhesive agent (sample D) and 0.1 wt% alginate hydrogel (sample H) at 25 °C, exhibited a shear-thinning behavior. Viscograms were fitted with a Carreau-Yasuda model. Correlation coefficient values were satisfactory for all the formulations. This model describes the shear-thinning behavior of polymer solutions or suspensions presenting two Newtonian plateaus for very low and very high shear rates, representing the low and high deformation states of hydrogels respectively.

At 25 °C, the major goal of this study was to evaluate if the hydrogel formulations could be applied by spraying. A pharmaceutical solution for spraying may exhibit a low viscosity at the steady state, presenting usually values $\eta < 200$ mPa-s at a shear rate around 340 s^{-1}. Thus, as we could observe in Figure 5, at 25 °C, all the mucoadhesive hydrogel formulations could be used for spraying applications.

The goal of flow rheometry studies at 37 °C was to investigate the texture and the hold of the hydrogel formulations once the $T_{sol–gel}$ was reached. The shear stress developed and associated to a stimulus for viscous liquids and foods seems to be constant and corresponds to shear rate values about 10 s^{-1} [29,97]. As observed in Figure 5, all the hydrogel formulations containing a mucoadhesive agent (samples F-K) exhibited, at 10 s^{-1} and 37 °C, viscosity values lower than the control value (sample D without mucoadhesive agent). These results, and according to viscoelastic properties previously described, suggested a partial loss on the crystalline structure of P407 micelles when mucoadhesive matrices are incorporated in the hydrogel. The formulations showing the closest behavior to P407-based hydrogels without mucoadhesive agent at 37 °C were the preparations containing the xanthan gum (at 0.05 and 0.1 wt%, samples J and K respectively) and sodium alginate (at 0.5 wt%, sample I).

3.4. Measurement of the Adhesive and Mucoadhesive Forces

Mucoadhesion is considered as a phenomenon creating an intimate contact between two surfaces, at least one of them being biological, remaining together for a prolonged period of time. In this context, it involves the intimate interaction between the dosage form and the mucosa. This contact is believed to be the result of the wetting and adsorption of hydrogels on the mucosa leading to the diffusion and interpenetration of hydrogel polymer chains with mucosal compounds. Therefore, polymer chains could establish supramolecular interactions with mucosa such as hydrogen bonds, electrostatic interaction or hydrophobic contacts.

The experimental method used and developed in this publication was inspired and modified from a previously described method by Ponchel [98,99]. This method is very useful, because more information can be reached in order to obtain different deformation parameters.

In a typical tensile experiment, the hydrogel was placed between the lower plate and the upper plate, covered or not with porcine gastric mucins. In these experiments, the force necessary to produce the detachment of the two surfaces was recorded as a function of the elongation distance between the upper surface and hydrogel formulation. In a typical force–elongation curve, several distinguished regions could be observed in Figure 6 [93,99].

The first part of the force–elongation curve (segment AB) corresponds to the force increase as a function of the elongation distance to reach the peak, corresponding to the maximal force required to detach the two surfaces (F_{max}). In this position of the curve, the contact surface between the hydrogel and the mucins, adsorbed on the upper plate (rheometer mobile), remained constant and is equal to the contact surface of the hydrogel. The second part of the curve corresponds to the segment BC, which will be the partial detachment period of the rheometer geometry from the hydrogel formulation. A slight decrease of the contact area is occurring. The final step of the curve (segment CD) indicates the total detachment of the mucin mobile from the lower support where the major change of the contact surface is occurring. Finally, the W part of the curve will correspond to the area under the curve leading to the adhesion work value (W_{adh}). The analysis of the whole

curve and not only the peak of detachment could give us some information about adhesive interactions between both materials. In this way, large deformation peaks would mean strong adhesive and more compliant interactions.

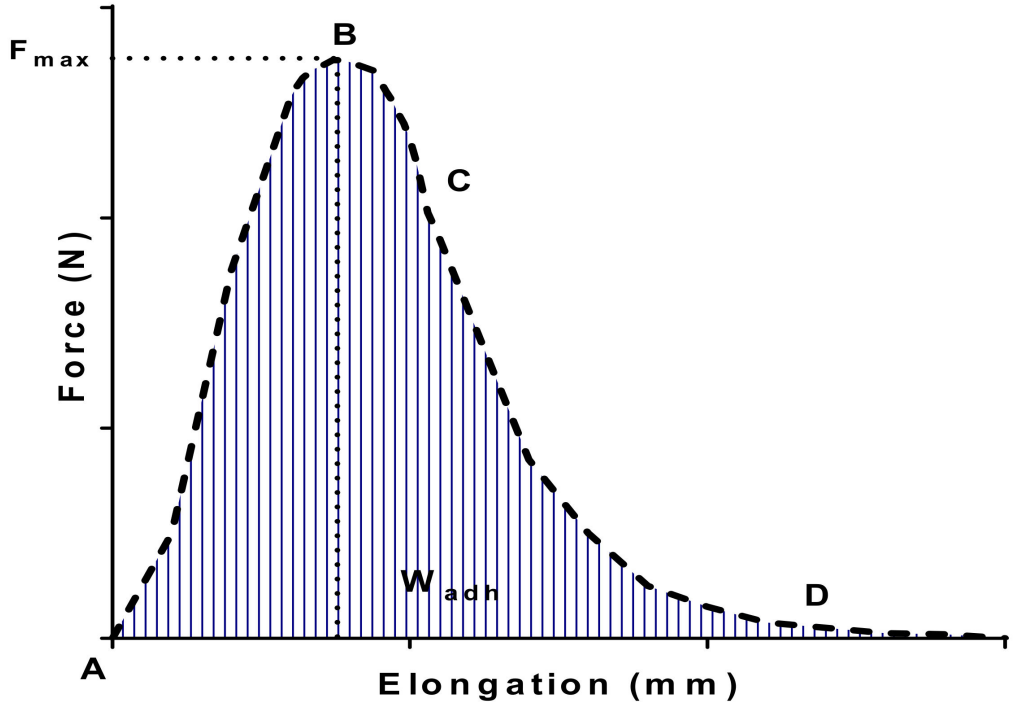


Figure 6. Typical force versus elongation curve for poloxamer P407-based hydrogels. The analysis of the curve can lead to the determination of the maximal force of detachment (F_{max}) and the work of adhesion (W_{adh}).

Comparing deformation parameters (F_{max} and W) in the presence and in absence of mucin, we observed a significant increase for those performed with mucins (Table 4). That indicates a positive interaction between hydrogels and mucins, which is coherent with data reported in the literature [46,48,50].

Table 4. Maximal force of detachment (F_{max}) and work of adhesion (W) values obtained from adhesion (adh) and mucoadhesion (m-adh) experiments at 37 °C using poloxamer P407-based hydrogels containing various mucoadhesive agents. The control sample consists of a solution of P407 in absence of mucoadhesive agent. ND: not determined, sample G exhibited. The values represented are the mean ± SD (n = 3).

Sample	Control Sample (D)	F	G	H	I	J	K
Mucoadhesive Agent	**- [b]**	**Carbopol C971P**		**Sodium Alginate**		**Xanthan Gum**	
Wt%	0	0.1	0.5	0.1	0.5	0.05	0.1
F_{adh} (N)	45.5 ± 1.2	42.9 ± 2.9	ND [a]	44.9 ± 2.8	53.1 ± 1.1	56.6 ± 6.5	58.2 ± 0.6
$F_{m\text{-}adh}$ (N)	60.9 ± 1.5	56.5 ± 2.0	ND [a]	79.7 ± 9.0	78.8 ± 5.9	66.2 ± 3.4	71.4 ± 2.9
W_{adh} (mJ)	2.2 ± 0.1	2.4 ± 0.2	ND [a]	3.4 ± 0.3	3.1 ± 0.5	2.5 ± 0.2	3.3 ± 0.2
$W_{m\text{-}adh}$ (mJ)	3.7 ± 0.3	3.2 ± 0.4	ND [a]	4.4 ± 0.6	3.6 ± 0.5	3.9 ± 0.3	4.6 ± 0.6

[a] ND: not determined, sample G exhibited an elastic behavior (solid-like) at room temperature. [b] without a mucoadhesive agent.

From the results reported in Figure 7, adhesion and mucoadhesion performed experiments confirmed that mucoadhesive agents included in the three-dimensional network of hydrogels were useful to increase the adhesive behavior of formulations, excepting the use of Carbopol (sample F).

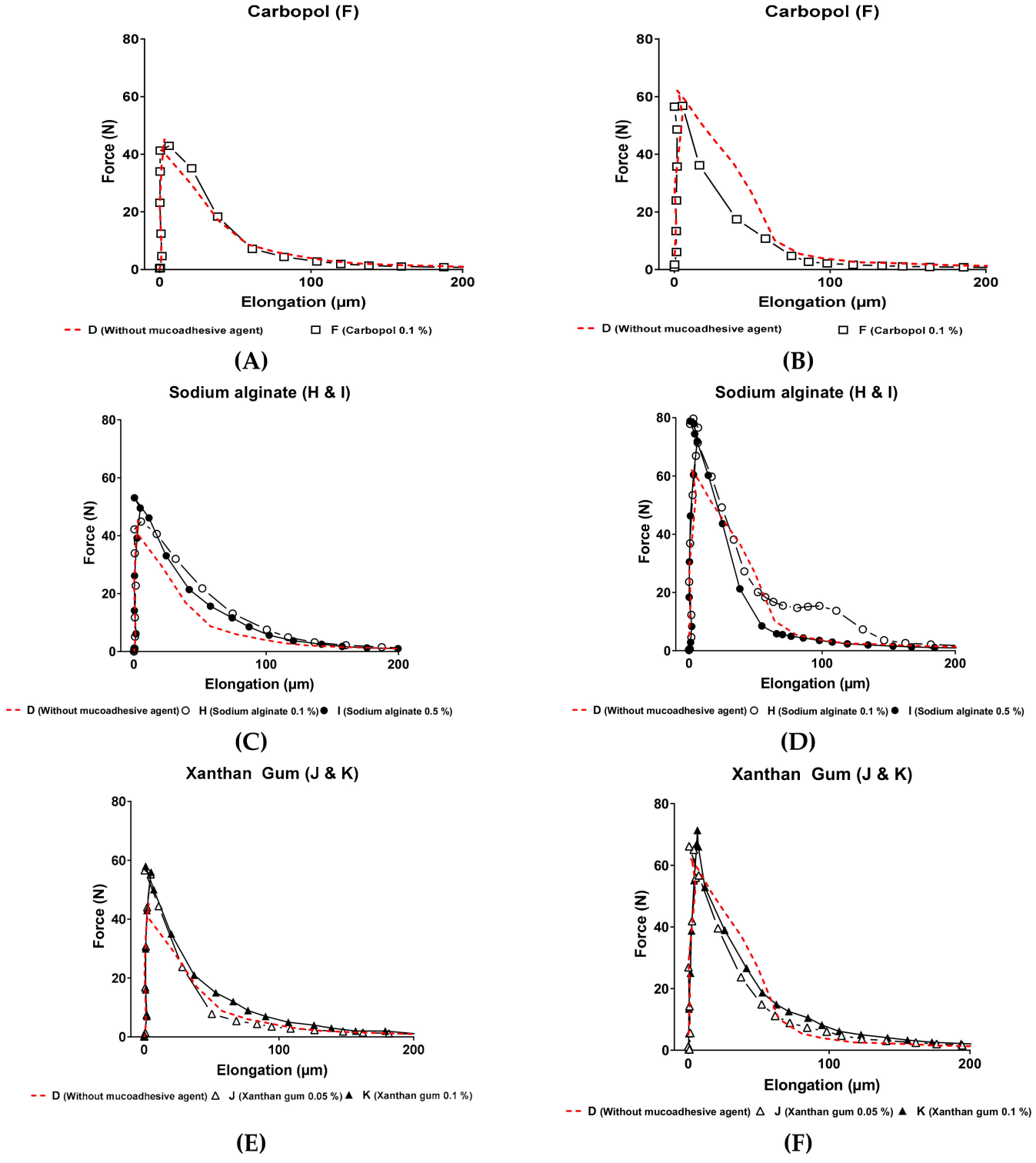


Figure 7. Forces curves as a function of elongation for Carbopol C971P sample F (**A**,**B**), sodium alginate samples H and I (**C**,**D**) and xanthan gum samples J and K (**E**,**F**). Force–elongation curves in the left side (**A**,**C**,**E**) correspond to adhesion profiles (without mucin). Curves in the right side correspond to mucoadhesion profiles (with mucin) (n = 3).

The control sample, prepared from a mucoadhesive agent-free P407-based hydrogel (sample D), exhibited more resistant deformation parameters than Carbopol C971P hydrogel preparations (sample F, p-value > 0.05 after a one-way ANOVA test). Nevertheless, we can observe that the maximal forces required to detach the upper plate from the mucoadhesive hydrogel containing sodium alginate (samples H and I) or xanthan gum (samples J and

K) were higher than the control sample (p-value < 0.05 for sodium alginate and xanthan gum hydrogel formulations). Despite maximal forces of detachment for xanthan gum being smaller than sodium alginate hydrogels, xanthan gum formulations seem to be slightly more mucoadhesive than sodium alginate regarding the work of adhesion. The higher elasticity (G' values at 37 °C) of P407-based hydrogels containing xanthan gum (samples J and K) could explain this difference, because the possibility of micelles to interact with mucin compounds would be increased. Furthermore, the increased viscosity at 37 °C of xanthan gum formulations, compared to sodium alginate (samples H and I) and Carbopol C971P (sample F), would increase the contact time between mucin and mucoadhesive agent, leading to a stronger mucoadhesive behavior.

3.5. Flow-Through USP-4 Apparatus In Vitro Drug Release

The main goal of this study was to establish an in vitro release test with mucoadhesive hydrogels allowing it to release 70–80% of the drug amount from the hydrogels within 30 min. This requirement comes from clinical demands to improve observance and efficacy of drug treatment. The in vitro release assay was performed in a liquid media mimicking physiological conditions in the oral cavity in terms of pH, salivary clearance and mechanical stress.

In this context, a simple exponential expression [100,101], as follows in the Equation (10), could be useful to analyze the controlled-release behavior of our hydrogels in the presence of xanthan gum at two different concentrations.

$$\frac{M_t}{M_\infty} = k \times t^n \tag{10}$$

where, M_t/M_∞ is the fractions of drug released (M_t is defined as the amount of drug released at time t and M_∞ is defined as the amount of drug released at time infinity), k is the kinetic constant, t is the release time and n is the diffusional exponent for drug release.

The diffusion exponent of this simple equation may give us some important information about the drug release mechanism [102]. In this context, and for a cylindrical matrix, if the exponent $n \leq 0.45$, then the drug release mechanism is the Fickian diffusion. Fickian diffusion involves the molecular diffusion of the drug due to a chemical potential gradient. If $n \geq 0.89$, then the drug is released by a case II transport, also called relaxational transport or erosion (typical zero order release). In this case, this phenomenon involves the penetration of the dissolution media into the polymer matrix at a controlled-rate modulating the drug release. Both phenomena are considered as the limiting case [71].

Many release processes, especially from hydrogels and swellable polymer matrices, are placed between the two limiting cases previously described: the simple diffusion and the erosion transport mechanism. In the case of both phenomena are coexisting, this case involves a diffusion exponent $0.45 < n < 0.89$ where the prevailing mechanism would a combination of simple diffusion and macromolecular relaxation because of the surrounding medium. For this reason, another equation may describe their drug release behavior from a thin polymer film, as follows:

$$\frac{M_t}{M_\infty} = k_1 t^{0.5} + k_2\, t \tag{11}$$

$$\frac{M_t}{M_\infty} = 4\left(\frac{D\, t}{\pi\, t^2}\right)^{0.5} = k_1 t^{0.5} \tag{12}$$

$$\frac{M_t}{M_\infty} = \frac{2\, k_0}{C_0\, l}\, t = k_2\, t \tag{13}$$

The first term of the Equation (11) corresponds to the Fickian contribution, where k_1 is the diffusion constant and represents the short-time approximation of the fractional drug released (Equation (12)) where D is the drug diffusion coefficient, l is the initial film thickness and t is the release time. The second term of the Equation (11) represents the relaxational contribution or erosion, where k_2 is the relaxation constant and defined as previously described in Equation (13) where k_o is the relaxation constant and C_o is the drug released concentration [100–102].

For further analysis of our data, a first fit of Equation (10) (expressing the drug release data versus time) was made for M_t/M_∞ up to 100% of the release as shown in Figure 8. As we can observe, DMA drug release from a P407-based hydrogel in the absence of a mucoadhesive agent was extremely high after a few minutes. Our strategy was to incorporate mucoadhesive polymers such as Carbopol C971P (sample F), sodium alginate (samples H and I) or xanthan gum (samples J and K) in order to slow down the release of DMA. As we can see in Figure 8, Carbopol C971P and sodium alginate showed release profiles very close to the mucoadhesive-free P407-based hydrogel (sample D). Regression parameters from the Korsmeyer–Peppas model showed a good fit (Table 5), meaning that the DMA release is mainly due to diffusion and in an immediate manner. The total amount of DMA was released over 10 min.

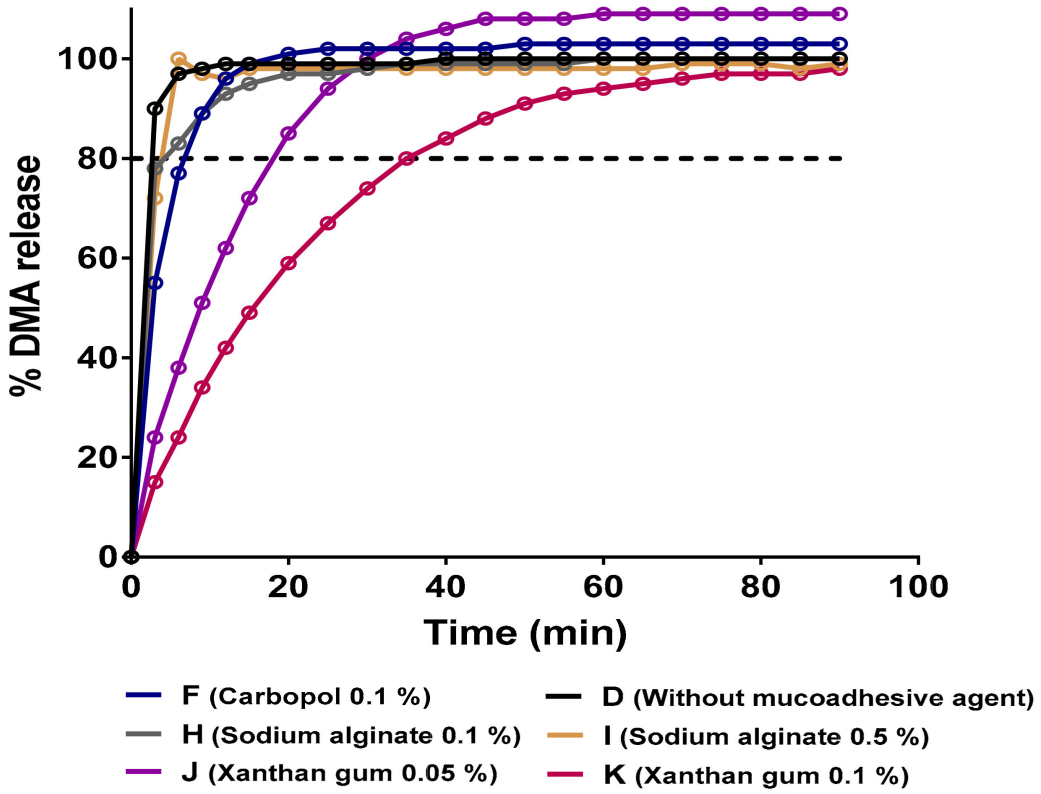


Figure 8. In vitro DMA (dexamethasone acetate) profiles from various hydrogels using the USP4 flow-through apparatus at 37 °C. The mean values of 3 experiments are represented.

Table 5. Mathematical model fitting of drug release data from formulations containing various mucoadhesive agents using the Korsmeyer–Peppas model (n = 3).

Sample			Korsmeyer–Peppas Fitted-Model			Short-Time Korsmeyer–Peppas Fitted-Model		
Code	**MA Agent**	**[C]**	**R^2 Adjusted**	**n**	**K**	**R^2 Adjusted**	**n**	**K**
Control	Ø	-	0.9953	0.015	93.5	ND [a]	ND [a]	ND [a]
F	Carbopol	0.1	0.9076	0.094	69.1	ND [a]	ND [a]	ND [a]
H	Alginate	0.1	0.9818	0.055	78.8	ND [a]	ND [a]	ND [a]
I	Alginate	0.5	0.9414	0.043	83.2	ND [a]	ND [a]	ND [a]
J	XG	0.05	*	*	*	0.999	0.76	7.6
K	XG	0.10	*	*	*	0.999	0.69	8.8

[a] ND: not determined, * Data not shown because of lack of fit for samples J and K.

However, one mucoadhesive compound was revealed as a promising agent, the xanthan gum (samples J and K). It is widely described in the scientific literature that xanthan gum can be used as an effective mucoadhesive agent to form a polymeric matrix enabling the extension of drug release [103]. An inverse relationship between the amount of xanthan gum present in the formulation and the drug release rate has been found [103,104]. In this case, the drug may be released at a constant rate pH-independent in a zero-order release guarantying a constant rate of drug release versus time [105]. The regression parameters of the Korsmeyer–Peppas fitted model were not good for released amounts of DMA up to 100%. Nevertheless, if fitted up to 60% of the total released amount of DMA (short time release), the correlation model was very high. At short times, up to 60% of total drug released, the n values are comprised between 0.45 and 0.89 indicating that two limiting phenomena, Fickian diffusion and erosion, are occurring in the hydrogel. A lower value of n for the higher concentration of xanthan gum indicates that a diffusion process is more predominant than for the lower concentration.

Regarding the second fitted-model data in Table 6, for short-times, we observed that for both formulations diffusion constants are higher than the relaxation contribution. When comparing both concentrations, we noted that diffusion is more important in 0.1% xanthan gum-based hydrogels (sample K) than formulations containing a lower concentration, sample J [103]. As well, for relaxation contribution, it is stronger for the 0.05% xanthan gum-based hydrogel.

Table 6. Mathematical model fitting of drug release data from formulations containing xanthan gum as mucoadhesive agent using Peppas–Sahlin model (n = 3).

Code	MA Agent	[C]	Peppas-Sahlin Fitted Model					
			Short-Time			Long-Time		
			K_1	**K_2**	**R^2 Adjusted**	**K_1**	**K_2**	**R^2 Adjusted**
J	XG	0.05	6.3	2.4	0.998	24.8	-	0.965
K	XG	0.10	8.5	1.6	0.994	24.3	-	0.992

Thus, xanthan gum may be an important compound controlling the drug release by diffusion phenomena and decreasing the relaxation of the hydrogel at short-time. If the experimental data were fitted to long-times, we realized that erosion mechanism did not exist anymore and the only phenomenon occurring was the Fickian diffusion.

A comparison of the release profiles of mucoadhesive-free P407-based hydrogel and those containing mucoadhesive compounds was performed with an independent-model analysis [106]. The f_1 (difference) and f_2 (similarity) factors were comprised between $0 \leq f_1 \leq 15$ and $50 \leq f_2 \leq 100$ respectively for all hydrogel formulations except those having xanthan gum as the mucoadhesive matrix. In that case, difference and similarity factor values were $f_1 > 15$ and $f_2 < 50$ respectively indicating that their dissolution profiles

were very different from the control sample. That confirms the effect of xanthan gum on the controlled-release profiles of P407-based hydrogel as previously suggested.

As previously described in the scientific literature, the surfaces of hydrogels tend to form a swollen layer to prevent a rapid penetration of the dissolution media, which may inhibit or limit the erosion of the formulation. In the other hand, sodium alginate, used as a controlled-release excipient (samples H and I) showed faster dissolution rates as previously described [107]. The potential presence of alginic acid molecules, due to slight variations on the pH, may act as a barrier for the media penetration. Those non-swellable properties could induce a strong erosion or dissolution of alginate-based hydrogels [104,107].

Based on Peppas–Sahlin fitted model (Figure 9) at short and long-times, the times for 25, 50, 80 and 90% of total released amount were calculated and the average values were shown in Table 7.

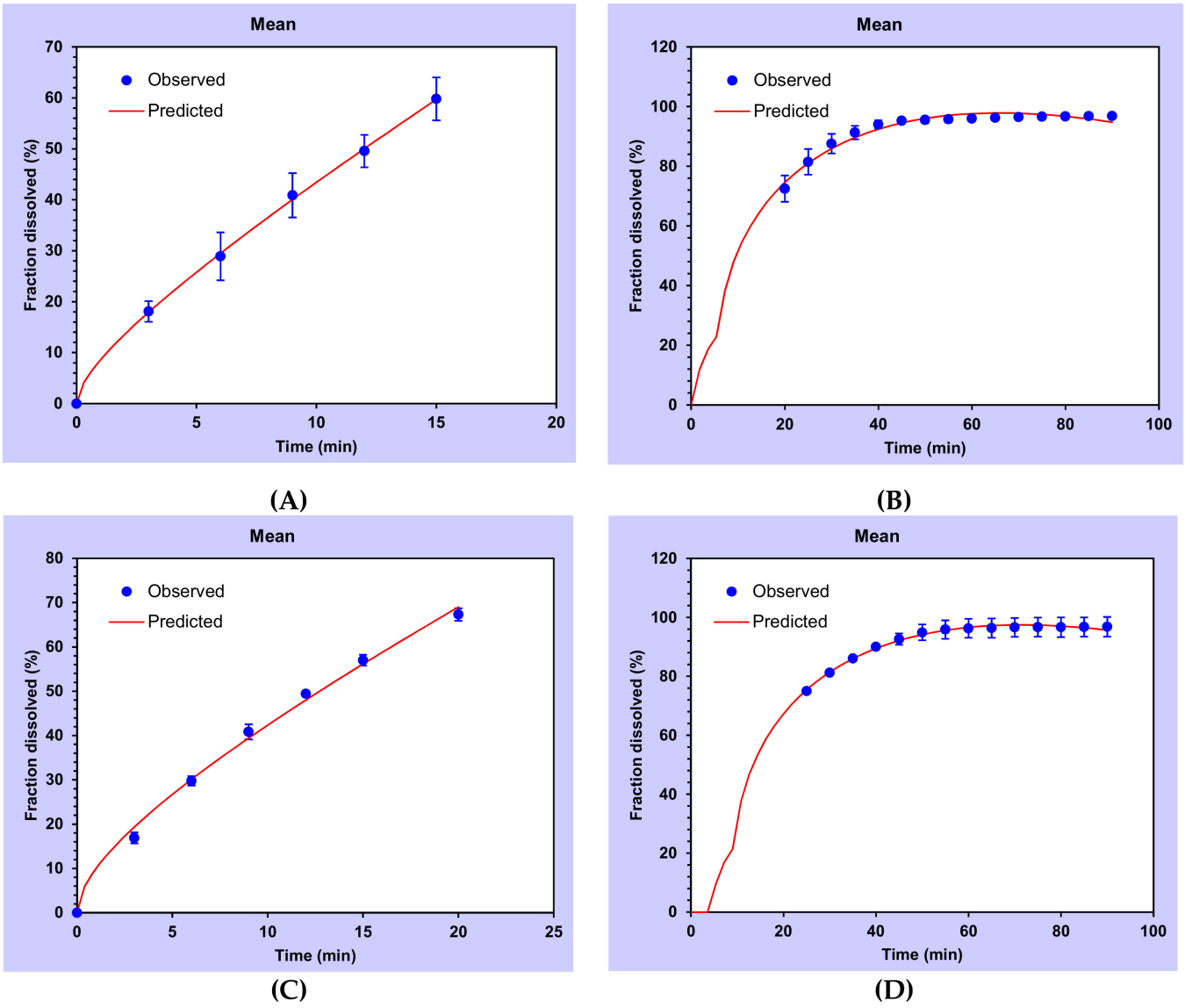


Figure 9. Drug release data fitted to a Peppas–Sahlin dissolution model. Short-times fit (**A**–**C**) and long-times fit (**B**–**D**) for poloxamer 407-based hydrogels containing xanthan gum at 0.05 (**A**–**B**) and 0.10 (**C**–**D**) wt% as a mucoadhesive agent.

Table 7. Times for 25, 50, 80 and 90% of drug release estimated from short- and long-times Peppas–Sahlin model for hydrogels containing xanthan gum as a mucoadhesive agent (n = 3).

Sample			Short-Times Drug Release Time (min)				Long-Times Drug Release Time (min)			
Code	**MA Agent**	**[C] (wt%)**	T_{25}	T_{50}	T_{80}	T_{90}	T_{25}	T_{50}	T_{80}	T_{90}
J	XG	0.05	4.8	12.0	21.5	24.9	4.6	9.1	24.0	35.5
K	XG	0.10	4.5	12.7.	24.6	28.8	8.3	13.0	28.6	41.2

4. Conclusions

Self-assembly of poloxamer 407 chains forming thermoresponsive hydrogels is still a promising approach to build new therapeutic mucosal and topical dosage forms using soft conditions without solvent, surfactants or any pH modifications. These hydrogels have been very useful for the treatment of topical or mucosal diseases by incorporating a therapeutic drug into the three dimensional network. However, its use is quite limited because of the lack of mucoadhesive properties. In this work, and in the context of the treatment of oral planus lichen, a chronic dermato-mucosal disease, we developed poloxamer P407-based hydrogels containing a poorly water soluble anti-inflammatory drug encapsulated into the cavity of HP-β-CD, dexamethasone acetate (DMA), with improved mucoadhesive behavior. Indeed, including mucoadhesive agents such as xanthan gum or sodium alginate increased significantly the adhesive properties of hydrogels. The effect of experimental formulations parameters, such as the poloxamer hydration ratio, presence of HP-β-CD and its state and the incorporation of mucoadhesive agents, on the rheological behavior was evaluated to identify key parameters.

Furthermore, in vitro drug release studies were performed. One of the mucoadhesive agents was identified as an in vitro controlling release compound. Xanthan gum, incorporated in the hydrogel formulation, was able to sustain drug release for longer times than the other compounds and the mucoadhesive-free hydrogel. This work opens the way to a new approach easing the design of mucoadhesive sprayable hydrogels for the treatment of mucosal diseases with water-insoluble drugs.

Author Contributions: R.D.-S. was responsible for validation, formal and statistical analysis, investigation, including dissolution profile analysis, data curation and writing the original draft preparation and review and editing. B.T. was responsible for methodology, data curation, data validation and writing review and editing. N.H. was responsible for validation as well as writing review and editing. E.B.D. and G.A. were responsible for methodology including preparation and physico-chemical characterization of hydrogels. H.H. and S.G.D. were responsible for validation, writing review and editing, formal analysis as well as data curation. A.D.W. and V.B. were both responsible for conceptualization, visualization, supervision, project administration, writing review and editing as well as funding acquisition. All authors have read and agreed to the published version of the manuscript.

Funding: This research received no external funding.

Institutional Review Board Statement: Not applicable.

Informed Consent Statement: Not applicable.

Data Availability Statement: Not applicable.

Acknowledgments: The authors acknowledge AGEPDS and AP-HP for structural and financial support to develop this work.

Conflicts of Interest: The authors declare no conflict of interest.

References

1. Boorghani, M.; Gholizadeh, N.; Zenouz, A.T.; Vatankhah, M.; Mehdipour, M. Oral lichen planus: Clinical features, etiology, treatment and management; a review of literature. *J. Dental Res. Dental Clin. Dental Prosp.* **2010**, *4*, 3. [CrossRef]
2. Gupta, S.; Jawanda, M.K. Oral lichen planus: An update on etiology, pathogenesis, clinical presentation, diagnosis and management. *Indian J. Dermatol.* **2015**, *60*, 222. [CrossRef] [PubMed]
3. Baek, K.; Choi, Y. The microbiology of oral lichen planus: Is microbial infection the cause of oral lichen planus? *Mol. Oral Microbiol.* **2018**, *33*, 22–28. [CrossRef] [PubMed]
4. Barnard, N.; Scully, C.; Eveson, J.; Cunningham, S.; Porter, S. Oral cancer development in patients with oral lichen planus. *J. Oral Pathol. Med.* **1993**, *22*, 421–424. [CrossRef] [PubMed]
5. Andreasen, J. Oral lichen planus: I. A clinical evaluation of 115 cases. *Oral Surg. Oral Med. Oral Pathol.* **1968**, *25*, 31–42. [CrossRef]
6. Scully, C.; El-Kom, M. Lichen planus: Review and update on pathogenesis. *J. Oral Pathol. Med.* **1985**, *14*, 431–458. [CrossRef]
7. McGrath, C.; Hegarty, A.M.; Hodgson, T.A.; Porter, S.R. Patient-Centred outcome measures for oral mucosal disease are sensitive to treatment. *Int. J. Oral Maxillofac. Surg.* **2003**, *32*, 334–336. [CrossRef]
8. Lozada, F.; Silverman, S. Topically applied fluocinonide in an adhesive base in the treatment of oral vesiculoerosive diseases. *Arch. Dermatol.* **1980**, *116*, 898–901. [CrossRef]
9. Holbrook, W.P.; Kristmundsdóttir, T.; Loftsson, T. Aqueous hydrocortisone mouthwash solution: Clinical evaluation. *Acta Odontol. Scand.* **1998**, *56*, 157–160. [CrossRef]
10. Hegarty, A.M.; Hodgson, T.A.; Lewsey, J.D.; Porter, S.R. Fluticasone propionate spray and betamethasone sodium phosphate mouthrinse: A randomized crossover study for the treatment of symptomatic oral lichen planus. *J. Am. Acad. Dermatol.* **2002**, *47*, 271–279. [CrossRef]
11. Aguirre, J.; Bagan, J.; Rodriguez, C.; Jimenez, Y.; Martínez-Conde, R.; Díaz de Rojas, F.; Ponte, A. Efficacy of mometasone furoate microemulsion in the treatment of erosive-ulcerative oral lichen planus: Pilot study. *J. Oral Pathol. Med.* **2004**, *33*, 381–385. [CrossRef] [PubMed]
12. Carbone, M.; Arduino, P.; Carrozzo, M.; Gandolfo, S.; Argiolas, M.; Bertolusso, G.; Conrotto, D.; Pentenero, M.; Broccoletti, R. Course of oral lichen planus: A retrospective study of 808 northern Italian patients. *Oral Dis.* **2009**, *15*, 235–243. [CrossRef] [PubMed]
13. Gonzalez-Moles, M.A.; Morales, P.; Rodriguez-Archilla, A.; Isabel, I.R.-A.; Gonzalez-Moles, S. Treatment of severe chronic oral erosive lesions with clobetasol propionate in aqueous solution. *Oral Surg. Oral Med. Oral Pathol. Oral Radiol. Endodontol.* **2002**, *93*, 264–270. [CrossRef] [PubMed]
14. Muzio, L.L.; Della Valle, A.; Mignogna, M.D.; Pannone, G.; Bucci, P.; Bucci, E.; Sciubba, J. The treatment of oral aphthous ulceration or erosive lichen planus with topical clobetasol propionate in three preparations: A clinical and pilot study on 54 patients. *J. Oral Pathol. Med.* **2001**, *30*, 611–617. [CrossRef]
15. Sardella, A.; Demarosi, F.; Oltolina, A.; Rimondini, L.; Carrassi, A. Efficacy of topical mesalazine compared with clobetasol propionate in treatment of symptomatic oral lichen planus. *Oral Dis.* **1998**, *4*, 255–259. [CrossRef]
16. Ungphaiboon, S.; Nittayananta, W.; Vuddhakul, V.; Maneenuan, D.; Kietthubthew, S.; Wongpoowarak, W. Phadoongsombat, N. Formulation and efficacy of triamcinolone acetonide mouthwash for treating oral lichen planus. *Am. J. Health Syst. Pharm.* **2005**, *62*, 485–491. [CrossRef]
17. González-Moles, M.A.; Scully, C. Vesiculo-Erosive Oral Mucosal Disease—Management with Topical Corticosteroids: (1) Fundamental Principles and Specific Agents Available. *J. Dent. Res.* **2005**, *84*, 294–301. [CrossRef]
18. Zakrzewska, J.; Chan, E.; Thornhill, M. A systematic review of placebo-controlled randomized clinical trials of treatments used in oral lichen planus. *Br. J. Dermatol.* **2005**, *153*, 336–341. [CrossRef]
19. Silverman, S.; Gorsky, M.; Lozada-Nur, F.; Giannotti, K. A prospective study of findings and management in 214 patients with oral lichen planus. *Oral Surg. Oral Med. Oral Pathol.* **1991**, *72*, 665–670. [CrossRef]
20. Thongprasom, K.; Dhanuthai, K. Steriods in the treatment of lichen planus: A review. *J. Oral Sci.* **2008**, *50*, 377–385. [CrossRef]
21. Zegarelli, D. Ulcerative and erosive lichen planus. Treated by modified topical steroid and injection steroid therapy. *N. Y. State Dent. J.* **1987**, *53*, 23–24. [PubMed]
22. Sankar, V.; Hearnden, V.; Hull, K.; Juras, D.V.; Greenberg, M.; Kerr, A.; Lockhart, P.; Patton, L.; Porter, S.; Thornhill, M. Local drug delivery for oral mucosal diseases: Challenges and opportunities: Local drug delivery for oral mucosal diseases. *Oral Dis.* **2011**, *1*, 73–84. [CrossRef] [PubMed]
23. Patel, R.S.; Poddar, S. Development and characterization of mucoadhesive buccal patches of salbutamol sulphate. *Curr. Drug Deliv.* **2009**, *6*, 140–144. [CrossRef] [PubMed]
24. Salamat-Miller, N.; Chittchang, M.; Johnston, T.P. The use of mucoadhesive polymers in buccal drug delivery. *Adv. Drug Deliv. Rev.* **2005**, *57*, 1666–1691. [CrossRef] [PubMed]
25. Singh, M.; Tiwary, A.; Kaur, G. Investigations on interpolymer complexes of cationic guar gum and xanthan gum for formulation of bioadhesive films. *Res. Pharm. Sci.* **2010**, *5*, 79–87. [PubMed]
26. Smart, J.D. Buccal drug delivery. *Expert opin. Drug Deliv.* **2005**, *2*, 507–517. [CrossRef]
27. Sun, B.; Wang, W.; He, Z.; Zhang, M.; Kong, F.; Sain, M. Biopolymer Substrates in Buccal Drug Delivery: Current Status and Future Trend. *Curr. Med. Chem.* **2020**, *27*, 1661–1669. [CrossRef]

28. Vasantha, P.V.; Puratchikody, A.; Mathew, S.T.; Balaraman, A.K. Development and characterization of Eudragit based mucoadhesive buccal patches of salbutamol sulfate. *Saudi Pharm. J.* **2011**, *19*, 207–214. [CrossRef]
29. Zeng, N.; Dumortier, G.; Maury, M.; Mignet, N.; Boudy, V. Influence of additives on a thermosensitive hydrogel for buccal delivery of salbutamol: Relation between micellization, gelation, mechanic and release properties. *Int. J. Pharm.* **2014**, *467*, 70–83. [CrossRef]
30. Zeng, N.; Seguin, J.; Destruel, P.-L.; Dumortier, G.; Maury, M.; Dhotel, H.; Bessodes, M.; Scherman, D.; Mignet, N.; Boudy, V. Cyanine derivative as a suitable marker for thermosensitive in situ gelling delivery systems: In vitro and in vivo validation of a sustained buccal drug delivery. *Int. J. Pharm.* **2017**, *534*, 128–135. [CrossRef]
31. Yu, S.; Zhang, X.; Tan, G.; Tian, L.; Liu, D.; Liu, Y.; Yang, X.; Pan, W. A novel pH-induced thermosensitive hydrogel composed of carboxymethyl chitosan and poloxamer cross-linked by glutaraldehyde for ophthalmic drug delivery. *Carbohydr. Polym.* **2017**, *155*, 208–217. [CrossRef] [PubMed]
32. Zeng, N.; Mignet, N.; Dumortier, G.; Olivier, E.; Seguin, J.; Maury, M.; Scherman, D.; Rat, P.; Boudy, V. Poloxamer bioadhesive hydrogel for buccal drug delivery: Cytotoxicity and trans-epithelial permeability evaluations using TR146 human buccal epithelial cell line. *Int. J. Pharm.* **2015**, *495*, 1028–1037. [CrossRef] [PubMed]
33. Al Sabbagh, C.; Seguin, J.; Agapova, E.; Kramerich, D.; Boudy, V.; Mignet, N. Thermosensitive hydrogels for local delivery of 5-fluorouracil as neoadjuvant or adjuvant therapy in colorectal cancer. *Eur. J. Pharm. Biopharm.* **2020**, *157*, 154–164. [CrossRef]
34. Hoare, T.R.; Kohane, D.S. Hydrogels in drug delivery: Progress and challenges. *Polymer* **2008**, *49*, 1993–2007. [CrossRef]
35. Peppas, N.; Bures, P.; Leobandung, W.; Ichikawa, H. Hydrogels in pharmaceutical formulations. *Eur. J. Pharm. Biopharm.* **2000**, *50*, 27–46. [CrossRef]
36. Koffi, A.A.; Agnely, F.; Ponchel, G.; Grossiord, J.L. Modulation of the rheological and mucoadhesive properties of thermosensitive poloxamer-based hydrogels intended for the rectal administration of quinine. *Eur. J. Pharm. Sci.* **2006**, *27*, 328–335. [CrossRef]
37. Singh, V.; Khullar, P.; Dave, P.N.; Kaur, N. Micelles, mixed micelles, and applications of polyoxypropylene (PPO)-polyoxyethylene (PEO)-polyoxypropylene (PPO) triblock polymers. *Int. J. Ind. Chem.* **2013**, *4*, 12. [CrossRef]
38. Sandri, G.; Cristina Bonferoni, M.; Ferrari, F.; Rossi, S.; Del Fante, C.; Perotti, C.; Gallanti, A.; Caramella, C. An in situ gelling buccal spray containing platelet lysate for the treatment of oral mucositis. *Curr. Drug Discov. Technol.* **2011**, *8*, 277–285. [CrossRef]
39. Dumortier, G.; Grossiord, J.L.; Agnely, F.; Chaumeil, J.C. A Review of Poloxamer 407 Pharmaceutical and Pharmacological Characteristics. *Pharm. Res.* **2006**, *23*, 2709–2728. [CrossRef]
40. Bochot, A.; Fattal, E.; Gulik, A.; Couarraze, G.; Couvreur, P. Liposomes dispersed within a thermosensitive gel: A new dosage form for ocular delivery of oligonucleotides. *Pharm. Res.* **1998**, *15*, 1364–1369. [CrossRef]
41. Henry, R. Burn wound coverings and the use of poloxamer preparations. *Crit. Rev. Biocompat.* **1989**, *5*, 207–220.
42. Morikawa, K.; Okada, F.; Hosokawa, M.; Kobayashi, H. Enhancement of therapeutic effects of recombinant interleukin 2 on a transplantable rat fibrosarcoma by the use of a sustained release vehicle, pluronic gel. *Cancer Res.* **1987**, *47*, 37–41. [PubMed]
43. Tomida, H.; Shinohara, M.; Kuwada, N.; Kiryu, S. In vitro release characteristics of diclofenac and hydrocortisone from Pluronic F-127 gels. *Acta Pharm. Suec.* **1987**, *24*, 263–272. [PubMed]
44. Chen, C.-C.; Fang, C.-L.; Al-Suwayeh, S.A.; Leu, Y.-L.; Fang, J.-Y. Transdermal delivery of selegiline from alginate—Pluronic composite thermogels. *Int. J. Pharm.* **2011**, *415*, 119–128. [CrossRef] [PubMed]
45. Hsu, S.-H.; Leu, Y.-L.; Hu, J.-W.; Fang, J.-Y. Physicochemical characterization and drug release of thermosensitive hydrogels composed of a hyaluronic acid/pluronic f127 graft. *Chem. Pharm. Bull.* **2009**, *57*, 453–458. [CrossRef] [PubMed]
46. Fefelova, N.A.; Nurkeeva, Z.S.; Mun, G.A.; Khutoryanskiy, V.V. Mucoadhesive interactions of amphiphilic cationic copolymers based on [2-(methacryloyloxy)ethyl]trimethylammonium chloride. *Int. J. Pharm.* **2007**, *339*, 25–32. [CrossRef] [PubMed]
47. Heemstra, L.B.; Finnin, B.C.; Nicolazzo, J.A. The Buccal Mucosa as an Alternative Route for the Systemic Delivery of Risperidone. *J. Pharm. Sci.* **2010**, *99*, 4584–4592. [CrossRef]
48. Russo, E.; Selmin, F.; Baldassari, S.; Gennari, C.G.M.; Caviglioli, G.; Cilurzo, F.; Minghetti, P.; Parodi, B. A focus on mucoadhesive polymers and their application in buccal dosage forms. *J. Drug Deliv. Sci. Technol.* **2016**, *32*, 113–125. [CrossRef]
49. Remuñán-López, C.; Portero, A.; Vila-Jato, J.L.; Alonso, M.J. Design and evaluation of chitosan/ethylcellulose mucoadhesive bilayered devices for buccal drug delivery. *J. Control. Release* **1998**, *55*, 143–152. [CrossRef]
50. Westhaus, E.; Messersmith, P.B. Triggered release of calcium from lipid vesicles: A bioinspired strategy for rapid gelation of polysaccharide and protein hydrogels. *Biomaterials* **2001**, *22*, 453–462. [CrossRef]
51. Menchicchi, B.; Fuenzalida, J.P.; Hensel, A.; Swamy, M.J.; David, L.; Rochas, C.; Goycoolea, F.M. Biophysical Analysis of the Molecular Interactions between Polysaccharides and Mucin. *Biomacromolecules* **2015**, *16*, 924–935. [CrossRef] [PubMed]
52. Roy, S.; Pal, K.; Anis, A.; Pramanik, K.; Prabhakar, B. Polymers in Mucoadhesive Drug-Delivery Systems: A Brief Note. *Des. Monomers Polym.* **2009**, *12*, 483–495. [CrossRef]
53. Mughal, M.A.; Iqbal, Z.; Neau, S.H. Guar Gum, Xanthan Gum, and HPMC Can Define Release Mechanisms and Sustain Release of Propranolol Hydrochloride. *AAPS PharmSciTech* **2011**, *12*, 77–87. [CrossRef] [PubMed]
54. Varshosaz, J.; Tavakoli, N.; Kheirolahi, F. Use of hydrophilic natural gums in formulation of sustained-release matrix tablets of tramadol hydrochloride. *AAPS PharmSciTech* **2006**, *7*, E168–E174. [CrossRef]
55. Verhoeven, E.; Vervaet, C.; Remon, J.P. Xanthan gum to tailor drug release of sustained-release ethylcellulose mini-matrices prepared via hot-melt extrusion: In vitro and in vivo evaluation. *Eur. J. Pharm. Biopharma.* **2006**, *63*, 320–330. [CrossRef]

56. Setterfield, J.; Black, M.; Challacombe, S. The management of oral lichen planus: Clinical dermatology—Review article. *Clin. Exp. Dermatol.* **2000**, *25*, 176–182. [CrossRef]
57. Thongprasom, K.; Luengvisut, P.; Wongwatanakij, A.; Boonjatturus, C. Clinical evaluation in treatment of oral lichen planus with topical fluocinolone acetonide: A 2-year follow-up. *J. Oral Pathol. Med.* **2003**, *32*, 315–322. [CrossRef]
58. Brewster, M.E.; Loftsson, T. Cyclodextrins as pharmaceutical solubilizers. *Adv. Drug Deliv. Rev.* **2007**, *59*, 645–666. [CrossRef]
59. Siegal, T.; Soti, F.; Biegon, A.; Pop, E.; Brewster, M.E. Effect of a chemical delivery system for dexamethasone (Dex-CDS) on peritumoral edema in an experimental brain tumor model. *Pharm. Res.* **1997**, *14*, 672–675. [CrossRef]
60. Aleem, O.; Kuchekar, B.; Pore, Y.; Late, S. Effect of β-cyclodextrin and hydroxypropyl β-cyclodextrin complexation on physicochemical properties and antimicrobial activity of cefdinir. *J. Pharm. Biomed. Anal.* **2008**, *47*, 535–540. [CrossRef]
61. Bibby, D.C.; Davies, N.M.; Tucker, I.G. Mechanisms by which cyclodextrins modify drug release from polymeric drug delivery systems. *Int. J. Pharm.* **2000**, *197*, 1–11. [CrossRef]
62. Criscuolo, G.R. The genesis of peritumoral vasogenic brain edema and tumor cysts: A hypothetical role for tumor-derived vascular permeability factor. *Yale J. Biol. Med.* **1993**, *66*, 277–314. [PubMed]
63. Brewster, M.; Loftsson, T. The use of chemically modified cyclodextrins in the development of formulations for chemical delivery systems. *Pharmazie* **2002**, *57*, 94–101.
64. Elmotasem, H.; Awad, G.E.A. A stepwise optimization strategy to formulate in situ gelling formulations comprising fluconazole-hydroxypropyl-beta-cyclodextrin complex loaded niosomal vesicles and Eudragit nanoparticles for enhanced antifungal activity and prolonged ocular delivery. *Asian J. Pharm. Sci.* **2019**, *15*, 617–636. [CrossRef] [PubMed]
65. Stella, V.J.; Rao, V.M.; Zannou, E.A.; Zia, V. Mechanisms of drug release from cyclodextrin complexes. *Adv. Drug Deliv. Rev.* **1999**, *36*, 3–16. [CrossRef]
66. Gavriloaia, M.-R.; Budura, E.-A.; Aramã, C.; Nitulescu, M.; Lupuleasa, D. Phase solubility studies and scanning electron microscopy of dexamethasone inclusion complexes with b-cyclodextrin and hydroxypropyl b-cyclodextrin. *Studia Univ. Vasile Goldis Seria Stiintele Vietii (Life Sci. Ser.)* **2012**, *22*, 83.
67. Koffi, A.; Agnely, F.; Besnard, M.; Brou, J.K.; Grossiord, J.; Ponchel, G. In vitro and in vivo characteristics of a thermogelling and bioadhesive delivery system intended for rectal administration of quinine in children. *Eur. J. Pharm. Biopharm.* **2008**, *69*, 167–175. [CrossRef]
68. Kristinsson, J.K.; Fridriksdóttir, H.; Thorisdottir, S.; Sigurdardottir, A.M.; Stefansson, E.; Loftsson, T. Dexamethasone-cyclodextrin-polymer co-complexes in aqueous eye drops. Aqueous humor pharmacokinetics in humans. *Invest. Ophthalmol. Vis. Sci.* **1996**, *37*, 1199–1203.
69. Higuchi, T.; Connors, K. Phase solubility diagram. *Adv. Anal. Chem. Instrum.* **1965**, *4*, 117–212.
70. Carreau, P.J. Rheological equations from molecular network theories. *Trans. Soc. Rheol.* **1972**, *16*, 99–127. [CrossRef]
71. Tang, J.; Srinivasan, S.; Yuan, W.; Ming, R.; Liu, Y.; Dai, Z.; Noble, C.O.; Hayes, M.E.; Zheng, N.; Jiang, W.; et al. Development of a flow-through USP 4 apparatus drug release assay for the evaluation of amphotericin B liposome. *Eur. J. Pharma. Biopharm.* **2019**, *134*, 107–116. [CrossRef] [PubMed]
72. Yuan, W.; Kuai, R.; Dai, Z.; Yuan, Y.; Zheng, N.; Jiang, W.; Noble, C.; Hayes, M.; Szoka, F.C.; Schwendeman, A. Development of a Flow-Through USP-4 Apparatus Drug Release Assay to Evaluate Doxorubicin Liposomes. *AAPS J.* **2017**, *19*, 150–160. [CrossRef] [PubMed]
73. Ju, H.L.; Liaw, S.-J. On the assessment of similarity of drug dissolution profiles—A simulation study. *Drug Inform. J. Drug Inform. Assoc.* **1997**, *31*, 1273–1289. [CrossRef]
74. Shah, V.P.; Tsong, Y.; Sathe, P.; Liu, J.-P. In vitro dissolution profile comparison—Statistics and analysis of the similarity factor, f2. *Pharm. Res.* **1998**, *15*, 889–896. [CrossRef]
75. Liu, J.-P.; Ma, M.-C.; Chow, S.-C. Statistical Evaluation of Similarity Factor f2 as a Criterion for Assessment of Similarity Between Dissolution Profiles. *Drug Inform. J.* **1997**, *31*, 1255–1271. [CrossRef]
76. Stevens, R.E.; Gray, V.; Dorantes, A.; Gold, L.; Pham, L. Scientific and Regulatory Standards for Assessing Product Performance Using the Similarity Factor, f2. *AAPS J.* **2015**, *17*, 301–306. [CrossRef]
77. Jansook, P.; Pichayakorn, W.; Muankaew, C.; Loftsson, T. Cyclodextrin-Poloxamer aggregates as nanocarriers in eye drop formulations: Dexamethasone and amphotericin B. *Drug Dev. Ind. Pharm.* **2016**, *42*, 1446–1454. [CrossRef]
78. Nogueiras-Nieto, L.; Alvarez-Lorenzo, C.; Sandez-Macho, I.; Concheiro, A.; Otero-Espinar, F.J. Hydrosoluble Cyclodextrin/Poloxamer Polypseudorotaxanes at the Air/Water Interface, in Bulk Solution, and in the Gel State. *J. Phys. Chem. B* **2009**, *113*, 2773–2782. [CrossRef]
79. Wenz, G.; Han, B.-H.; Müller, A. Cyclodextrin rotaxanes and polyrotaxanes. *Chem. Rev.* **2006**, *106*, 782–817. [CrossRef]
80. Kesavan, K.; Kant, S.; Singh, P.N.; Pandit, J.K. Effect of Hydroxypropyl-β-cyclodextrin on the Ocular Bioavailability of Dexamethasone from a pH-Induced Mucoadhesive Hydrogel. *Curr. Eye Res.* **2011**, *36*, 918–929. [CrossRef]
81. Echezarreta-López, M.; Vila-Jato, J.; Torres-Labandeira, J. *The Effects of Cyclodextrins on the Incompatibility Dexamethasone-Polymyxin B in Solution*; Springer: Berlin/Heidelberg, Germany, 1996; pp. 457–460.
82. Liu, X.-M.; Lee, H.-T.; Reinhardt, R.A.; Marky, L.A.; Wang, D. Novel biomineral-binding cyclodextrins for controlled drug delivery in the oral cavity. *J. Control. Release* **2007**, *122*, 54–62. [CrossRef] [PubMed]
83. Turnbull, W.B.; Daranas, A.H. On the Value of *c*: Can Low Affinity Systems Be Studied by Isothermal Titration Calorimetry? *J. Am. Chem. Soc.* **2003**, *125*, 14859–14866. [CrossRef] [PubMed]

84. Haimhoffer, Á.; Rusznyák, Á.; Réti-Nagy, K.; Vasvári, G.; Váradi, J.; Vecsernyés, M.; Bácskay, I.; Fehér, P.; Ujhelyi, Z.; Fenyvesi, F. Cyclodextrins in Drug Delivery Systems and Their Effects on Biological Barriers. *Sci. Pharm.* **2019**, *87*, 33. [CrossRef]
85. Mazzaferro, S.; Bouchemal, K.; Gallard, J.-F.; Iorga, B.I.; Cheron, M.; Gueutin, C.; Steinmesse, C.; Ponchel, G. Bivalent sequential binding of docetaxel to methyl-β-cyclodextrin. *Int. J. Pharm.* **2011**, *416*, 171–180. [CrossRef] [PubMed]
86. Pradines, B.; Gallard, J.-F.; Iorga, B.I.; Gueutin, C.; Ponchel, G.; Loiseau, P.M.; Bouchemal, K. The unexpected increase of clotrimazole apparent solubility using randomly methylated β-cyclodextrin: Clotrimazole Solubility Increase. *J. Mol. Recognit.* **2015**, *28*, 96–102. [CrossRef]
87. Mateen, R.; Hoare, T. Carboxymethyl and hydrazide functionalized β-cyclodextrin derivatives: A systematic investigation of complexation behaviours with the model hydrophobic drug dexamethasone. *Int. J. Pharm.* **2014**, *472*, 315–326. [CrossRef]
88. Beig, A.; Agbaria, R.; Dahan, A. Oral Delivery of Lipophilic Drugs: The Tradeoff between Solubility Increase and Permeability Decrease when Using Cyclodextrin-Based Formulations. *PLoS ONE* **2013**, *8*, e68237. [CrossRef]
89. Usayapant, A.; Karara, A.H.; Narurkar, M.M. Effect of 2-hydroxypropyl-β-cyclodextrin on the ocular absorption of dexamethasone and dexamethasone acetate. *Pharm. Res.* **1991**, *8*, 1495–1499. [CrossRef]
90. Castillo, J.; Palomo-Canales, J.; Garcia, J.; Lastres, J.; Bolas, F.; Torrado, J. Preparation and characterization of albendazole β-cyclodextrin complexes. *Drug Dev. Ind. Pharm.* **1999**, *25*, 1241–1248. [CrossRef]
91. Thakur, A.; Kadam, R.S.; Kompella, U.B. Influence of Drug Solubility and Lipophilicity on Transscleral Retinal Delivery of Six Corticosteroids. *Drug Metab. Dispos.* **2011**, *39*, 771–781. [CrossRef]
92. Zoubari, G.; Staufenbiel, S.; Volz, P.; Alexiev, U.; Bodmeier, R. Effect of drug solubility and lipid carrier on drug release from lipid nanoparticles for dermal delivery. *Eur. J. Pharm. Biopharm.* **2017**, *110*, 39–46. [CrossRef] [PubMed]
93. Aka-Any-Grah, A.; Bouchemal, K.; Koffi, A.; Agnely, F.; Zhang, M.; Djabourov, M.; Ponchel, G. Formulation of mucoadhesive vaginal hydrogels insensitive to dilution with vaginal fluids. *Eur. J. Pharm. Biopharm.* **2010**, *76*, 296–303. [CrossRef] [PubMed]
94. Choi, H.-G.; Lee, M.-K.; Kim, M.-H.; Kim, C.-K. Effect of additives on the physicochemical properties of liquid suppository bases. *Int. J. Pharm.* **1999**, *190*, 13–19. [CrossRef]
95. Ur-Rehman, T.; Tavelin, S.; Gröbner, G. Effect of DMSO on micellization, gelation and drug release profile of Poloxamer 407. *Int. J. Pharm.* **2010**, *394*, 92–98. [CrossRef] [PubMed]
96. Lemdani, K.; Seguin, J.; Lesieur, C.; Al Sabbagh, C.; Doan, B.-T.; Richard, C.; Capron, C.; Malafosse, R.; Boudy, V.; Mignet, N. Mucoadhesive thermosensitive hydrogel for the intra-tumoral delivery of immunomodulatory agents, in vivo evidence of adhesion by means of non-invasive imaging techniques. *Int. J. Pharm.* **2019**, *567*, 118421. [CrossRef] [PubMed]
97. Shama, F.; Sherman, P. Identification of stimuli controlling the sensory evaluation of viscosity II. Oral methods. *J. Texture Stud.* **1973**, *4*, 111–118. [CrossRef]
98. Lejoyeux, F. Evaluation de la Bioadhésion de systemes Matriciels D'acide Polyacrylique: Influence de Paramètres Physicochimiques et Pharmacotechniques. Ph.D. Thesis, University of Paris, Paris, France, 1991.
99. Ponchel, G.; Touchard, F.; Duchêne, D.; Peppas, N.A. Bioadhesive analysis of controlled-release systems. I. Fracture and interpenetration analysis in poly (acrylic acid)-containing systems. *J. Control. Release* **1987**, *5*, 129–141. [CrossRef]
100. Ritger, P.L.; Peppas, N.A. A simple equation for description of solute release II. Fickian and anomalous release from swellable devices. *J. Control. Release* **1987**, *5*, 37–42. [CrossRef]
101. Ritger, P.L.; Peppas, N.A. A simple equation for description of solute release I. Fickian and non-fickian release from non-swellable devices in the form of slabs, spheres, cylinders or discs. *J. Control. Release* **1987**, *5*, 23–36. [CrossRef]
102. Peppas, N.A.; Sahlin, J.J. A simple equation for the description of solute release. III. Coupling of diffusion and relaxation. *Int. J. Pharm.* **1989**, *57*, 169–172. [CrossRef]
103. Kar, R.; Mohapatra, S.; Bhanja, S.; Das, D.; Barik, B. Formulation and in vitro characterization of xanthan gum-based sustained release matrix tables of isosorbide-5-mononitrate. *Iranian J. Pharm. Res.* **2010**, *9*, 13.
104. Talukdar, M.M.; Plaizier-Vercammen, J. Evaluation of xanthan cum as a hydrophilic matrix for controlled-release dosage form preparations. *Drug Dev. Ind. Pharm.* **1993**, *19*, 1037–1046. [CrossRef]
105. Andreopoulos, A.; Tarantili, P. Xanthan gum as a carrier for controlled release of drugs. *J. Biomater. Appl.* **2001**, *16*, 34–46. [CrossRef] [PubMed]
106. Boddeda, B.; Kumari, P.K.; Chowdary, K. Formulation and evaluation of glipizide sustained release tablets. *Int J. Pharm. Biomed. Res.* **2012**, *3*, 44–48.
107. Lu, M.F.; Woodward, L.; Borodkin, S. Xanthan gum and alginate based controlled release theophylline formulations. *Drug Dev. Ind. Pharm.* **1991**, *17*, 1987–2004. [CrossRef]